

AD_____

Award Number: W81XWH-10-1-0520

TITLE: Preclinical Studies of Induced Pluripotent Stem Cell-Derived Astrocyte Transplantation in ALS

PRINCIPAL INVESTIGATOR: Nicholas J. Maragakis, M.D.

CONTRACTING ORGANIZATION: Johns Hopkins University, School of Medicine
Baltimore, MD 21205

REPORT DATE: October 2013

TYPE OF REPORT: Annual

PREPARED FOR: U.S. Army Medical Research and Materiel Command
Fort Detrick, Maryland 21702-5012

DISTRIBUTION STATEMENT: Approved for Public Release;
Distribution Unlimited

The views, opinions and/or findings contained in this report are those of the author(s) and should not be construed as an official Department of the Army position, policy or decision unless so designated by other documentation.

REPORT DOCUMENTATION PAGE

*Form Approved
OMB No. 0704-0188*

Public reporting burden for this collection of information is estimated to average 1 hour per response, including the time for reviewing instructions, searching existing data sources, gathering and maintaining the data needed, and completing and reviewing this collection of information. Send comments regarding this burden estimate or any other aspect of this collection of information, including suggestions for reducing this burden to Department of Defense, Washington Headquarters Services, Directorate for Information Operations and Reports (0704-0188), 1215 Jefferson Davis Highway, Suite 1204, Arlington, VA 22202-4302. Respondents should be aware that notwithstanding any other provision of law, no person shall be subject to any penalty for failing to comply with a collection of information if it does not display a currently valid OMB control number. PLEASE DO NOT RETURN YOUR FORM TO THE ABOVE ADDRESS.

1. REPORT DATE October 2013	2. REPORT TYPE Annual	3. DATES COVERED 30 September 2012– 29 September 2013		
4. TITLE AND SUBTITLE Preclinical Studies of Induced Pluripotent Stem Cell-Derived Astrocyte Transplantation in ALS			5a. CONTRACT NUMBER	
			5b. GRANT NUMBER W81XWH-10-1-0520	
			5c. PROGRAM ELEMENT NUMBER	
6. AUTHOR(S) Nicholas J. Maragakis, M.D., Hongjun Song, Ph.D. E-Mail: nmaragak@jhmi.edu			5d. PROJECT NUMBER	
			5e. TASK NUMBER	
			5f. WORK UNIT NUMBER	
7. PERFORMING ORGANIZATION NAME(S) AND ADDRESS(ES) Johns Hopkins University, School of Medicine Baltimore, MD 21205			8. PERFORMING ORGANIZATION REPORT NUMBER	
9. SPONSORING / MONITORING AGENCY NAME(S) AND ADDRESS(ES) U.S. Army Medical Research and Materiel Command Fort Detrick, Maryland 21702-5012			10. SPONSOR/MONITOR'S ACRONYM(S)	
			11. SPONSOR/MONITOR'S REPORT NUMBER(S)	
12. DISTRIBUTION / AVAILABILITY STATEMENT Approved for Public Release; Distribution Unlimited				
13. SUPPLEMENTARY NOTES				
14. ABSTRACT We have made substantial progress in obtaining skin biopsies with subsequent fibroblast cultures of a number of sporadic ALS, familial ALS, and control subjects in the last year. We have created numerous iPS cell lines from these patient samples and have characterized their long-term differentiation into astroglia. We now have data from the <i>in vivo</i> transplantation of these astroglial progenitors into rat spinal cords. We have characterized several control and 1 ALS cell line with regard to their survival, differentiation, migration, and phenotypic effects on the host animals. Our data demonstrate that there are differences amongst the cell lines with regard to these properties but we have not appreciated obvious differences with regard to ALS cells when compared with control astroglial cells. Finally, we have demonstrated, in preparation for our therapeutic approaches, that these glial progenitor cells continue to mature into astrocytes following transplantation but that their survival is significantly reduced when compared with previous studies using human fatally-derived glial restricted precursors.				
15. SUBJECT TERMS Stem Cells, iPS cells, astrocytes, familial ALS				
16. SECURITY CLASSIFICATION OF:		17. LIMITATION OF ABSTRACT UU	18. NUMBER OF PAGES 56	19a. NAME OF RESPONSIBLE PERSON USAMRMC
a. REPORT U	b. ABSTRACT U	c. THIS PAGE U		19b. TELEPHONE NUMBER (include area code)

Table of Contents

	<u>Page</u>
Introduction.....	3
BODY.....	3-7
Key Research Accomplishments.....	8
Reportable Outcomes.....	8
Conclusion.....	8
References.....	8
Appendices.....	9

INTRODUCTION:

The overall objective is to examine whether human iPSC-GRPs (glial restricted precursors) derived from either sporadic ALS, familial (SOD1-mediated) ALS, or control subjects have the same capacity for engraftment, survival, and neuroprotective qualities following transplantation. It is not known whether iPSC-GRPs from ALS patients will in fact be normal (and thus possibly neuroprotective) or whether these iPSC-derived cells may in fact harbor ALS-specific abnormalities that may lack benefit or, potentially exacerbate disease. By comparing normal iPSC-GRPs with sALS iPSC-GRPs and fALS iPSC-GRPs we will also learn about inherent differences in astrocyte biology related to ALS, which will provide potential insights into disease mechanisms.

BODY:

Aim #1. Generation of human induced pluripotent stem cell-derived glial restricted precursors (iPSC-GRPs) from ALS subject fibroblasts

1. Fibroblast and iPSC lines from subjects with ALS and controls

Total of approximately 119 subjects biopsied to date). These include subjects with familial ALS (these include SOD1, ANG, FIG4, FUS, C9ORF72, and VCP mutations), as well as subjects with sporadic ALS and control subjects.

KNOWN FAMILIAL MUTATIONS	FIBROBLASTS	iPS
SOD1		
A4V	6	x
C38G	1	x
E49K	1	x
G85R	1	x
A89V	1	x
D90A	3	x
E100G	1	x
I112T	1	x
I113T	4	x
N139K	1	x
L144F/S?	1	x
V148G	1	x
FUS		
66 unkn var	1	x
H517Q	1	x
R522R	1	x
ANG	1	x
C9ORF72	9	x
FIG 4 unkn var	1	x
TDP43	2	
VCP (pre-symp)	1	x
TOTAL	38	27

OTHER	
SPORADIC	fibro
SLOW PROGRESSING > 5 YRS	20
RAPID PROGRESSION < 2 YRS	5
TYPICAL PROGRESSION 2-5 YRS	21
ALS/FTD	4
UNKNOWN FAMILIAL	3
PLS	10
LMN ONLY	6
UMN ONLY	1
PSEUDO BULBAR	1
KENNEDY'S	3
CONTROLS	6
RELATED CONTROLS	3
TOTAL	83

iPS lines completed	
fALS	28
sporadic ALS	18
other	6
controls	7
TOTAL	59

2. Sharing of iPSC lines with collaborators. Central to the ALSRP mission has been to generate human iPSC from a variety of ALS subjects. We have continued to expand on this effort. We have now sent iPSCs from control and ALS lines to the following institutions:

Thomas Jefferson University (Trotti and Pasinelli, PIs)
 Thomas Jefferson University (Lepore, PI)
 University of California, San Diego (Yeo, PI)
 University of California, San Diego (Cleveland)
 University of Milan, Italy (Corti, PI)
 NINDS, (Fischbeck, PI)
 Louisiana State University (Pandey, PI)
 Columbia University (Maniatis, PI)
 Harvard University (Eggan, PI)

3. Differentiation of iPSCs into astrocytes.

We have now initiated an in vitro evaluation of iPSC-derived astrocytes to ascertain whether they express appropriate astrocytic markers including GFAP, the astrocyte-specific glutamate transporter GLT1, connexin 43, aquaporin 4, the cell surface marker CD44 (a marker of astrocyte precursor identity), and the intermediate filament vimentin. Our data do not indicate differences in the capacity for differentiation between SOD1 ALS and control astrocytes (**Fig. 1**). Similar differentiation protocols have also been demonstrated for other non-SOD1 genotypes including C9ORF72 (*not shown*).

Figure 1. Differentiation of SOD1-iPSCs to astroglia. Representative pictures of control (006) and SOD1-iPSC (008) derived astrocyte after 15-week differentiation showing astrogial marker expression. (A) CD44 (red) and GFAP (green) expression by differentiated cells. Thin arrows indicate GFAP+ cells. Arrowheads indicate CD44+ cells. Thick arrows indicate CD44+/GFAP+ cells. (B) Quantification of CD44+ and GFAP+ cells at different time points. (C) EAAT1 (red) expression by GFAP+ (green) astrocytes. Arrows indicate double positive cells. (D) Aquaporin 4 (AQ4, red) and EAAT2 (green) expression. Nuclei were stained with DAPI (blue). Size bar, 20 μ m.

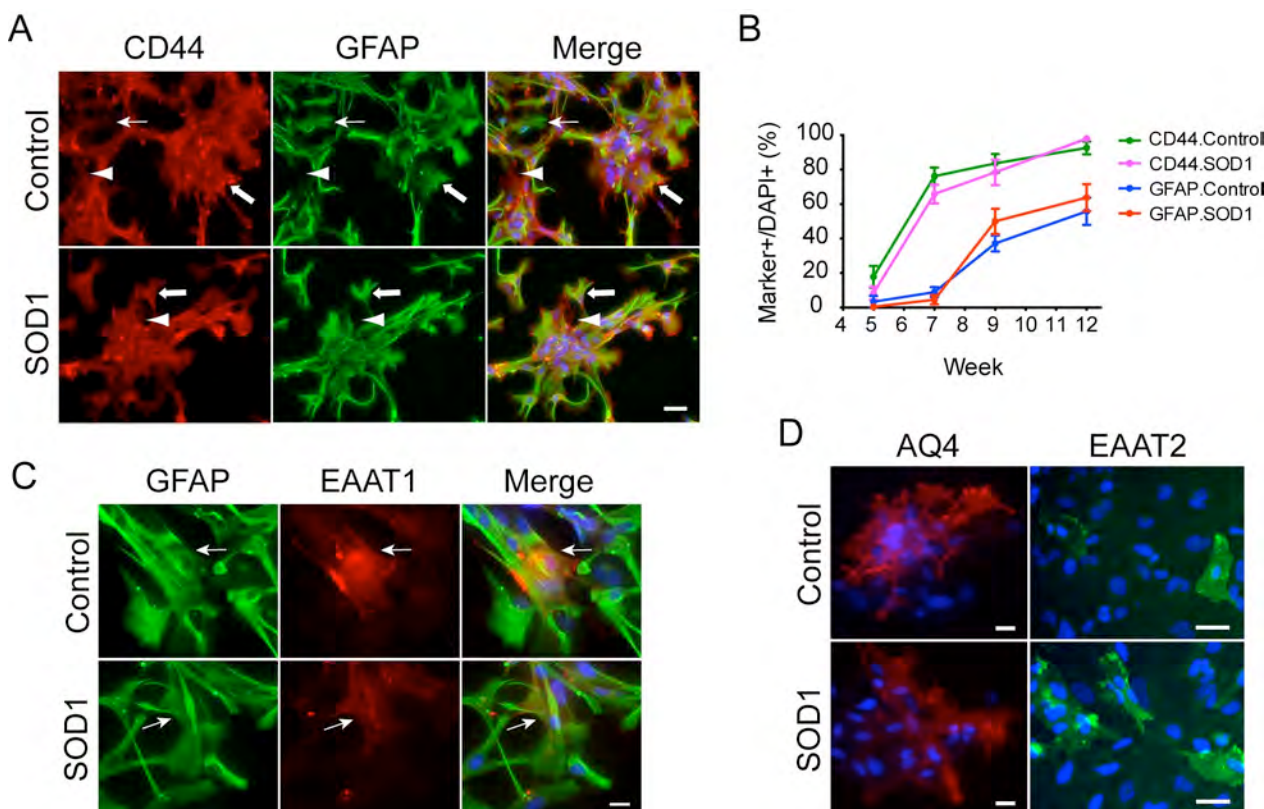


Figure 1

4. The demonstration of normal karyotype following multiple passages (Figure 2).

One fundamental concern for the use of iPSC-derived astrocytes for in vitro analyses or cell therapeutics is the fidelity of the resulting line following multiple passages. Here we show the karyotypes of fALS-iPS cells. The iPS cells were analyzed between passage number 4 to 10 (P4 – P10). Line 010 showed balanced translocation due to reciprocal exchange between the long-arm of chromosome 1 and the short-arm of chromosome 17. This line (010) will be removed from the library of available cells for future use.

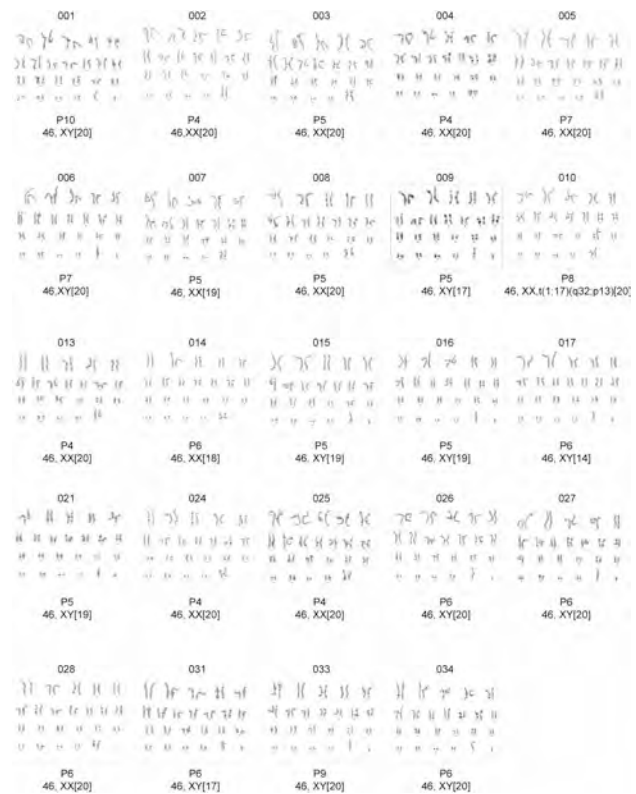


Figure 2

Significance: Our data demonstrate that we have derived a comprehensive list of iPSC from control, familial ALS, and sporadic ALS patients. We also demonstrate that they are karyotypically normal after numerous passages (or will be removed) and that they can be differentiated into astrocyte precursors independent of the presence of SOD1 mutations.

Aim #2. In vivo comparison of iPS cell-derived glial restricted precursors (iPSC-GRPs) from control, sporadic ALS, and familial ALS (SOD1) following transplantation into wildtype spinal cord

1. The detailed characterization of these lines is contained in the manuscript under revision titled: “Gene profiling of human iPSC-derived astrocyte progenitors following spinal cord engraftment”. A current version of this is located in the Appendix.

2. iPSC-Derived GRPs from FUS H517Q ALS do not significantly differ from control iPSC-derived GRP lines

One question is whether iPSC-derived GRPs from ALS subjects will have different properties when compared with control iPSC-derived GRPs. This has important implications for cell therapeutics since several current human ALS “stem cell” trials internationally have relied on the harvesting of host stem cells.

To begin to address this we used a transplantation paradigm from a FUS ALS line (Line AB025).

Significance: Our initial data using the familial ALS FUS line FUS^{H517Q} would not indicate an inherent toxicity from the presence of this mutation and could suggest that (at least for FUS ALS), that autologous transplantation of iPSC-derived GRPs could be a safe neuroprotective strategy.

Figure 3. The FUS^{H517Q} ALS line does not have a significant difference in its capacity for differentiation into astrocyte phenotypes when compared with control (H13, 11a, 18c) lines in vitro.

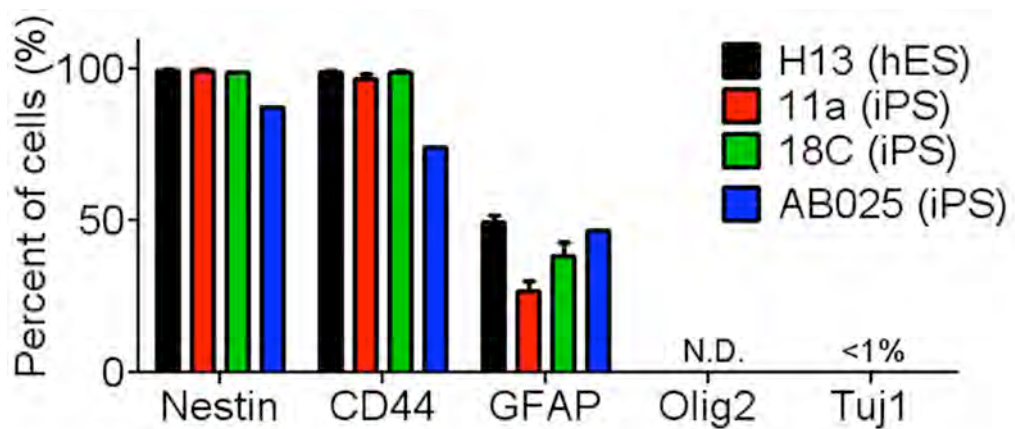


Figure 4: 12 weeks following spinal cord transplantation into the rat, the FUS^{H517Q} ALS line does not have a significant difference in its capacity for differentiation into astrocyte phenotypes when compared with control (H13, 11a, 18c) lines in vivo. The majority of these cells differentiate into GFAP+ astrocytes with few (Olig2+) oligodendrocytes.

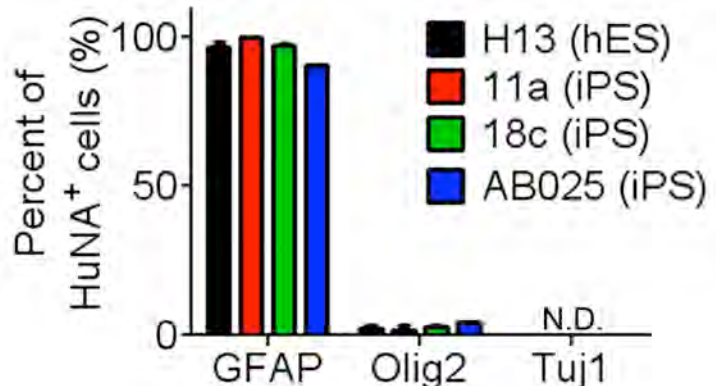


Figure 5: 12 weeks following spinal cord transplantation into the rat, the FUS^{H517Q} ALS line does not have a significant difference in its capacity for migration when compared with control (H13, 11a, 18c) lines in vivo. The capacity for migration in all 4 lines is limited.

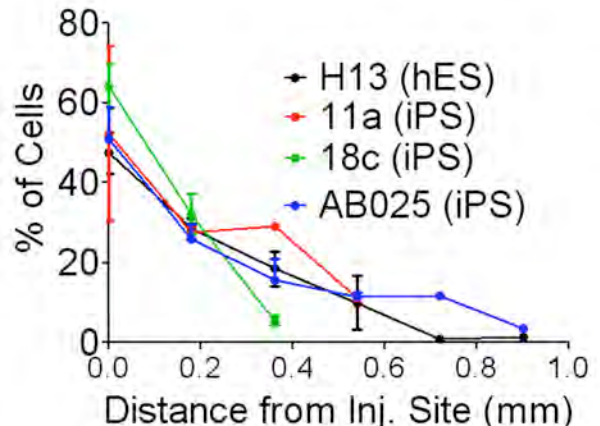
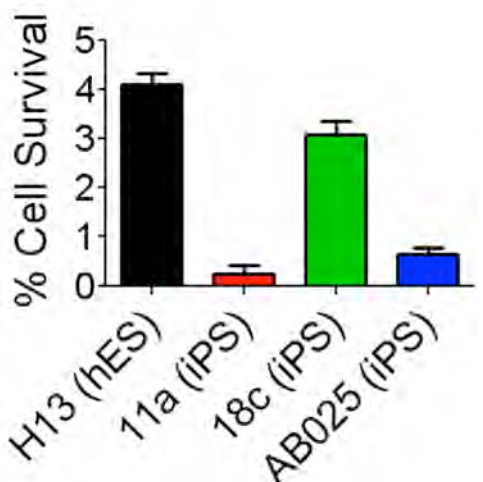


Figure 6: Following in vivo transplantation, there is limited survival of all iPSC-derived GRP subtypes including the FUS^{H517Q} ALS line AB025. We did not appreciate any host (WT rat) motor neuron death following the transplantation of the AB025 line (not shown).



Aim #3. Determine the capacity for neuroprotection of iPSC-derived glial restricted precursors (iPSC-GRPs) following transplantation into the SOD1^{G93A} rat model of ALS.

1. Analysis of most appropriate lines for preclinical study of iPSC-derived astrocyte progenitor cell therapies. Given the poor survival of the majority of our human iPSC-derived glial progenitors, our initial data suggested that the transplantation paradigm (including the immunosuppression strategy, sites of transplantation, numbers of cells, etc.) would not provide adequate neuroprotection and the properties of the iPSC-glial progenitor lines appeared distinct from our previous description of both rat and human fetally-derived glial progenitors.

However, we have more recently characterized a control line of iPSC which has unique properties from those described above. It appears that these cells are less differentiated and have the capacity to express both astrocyte and oligodendrocyte genes. They appear to have an improved capacity for both survival and migration (the reason for this is not yet entirely evident).

Astrocytes derived from the ciPS cell line resulted in much improved survival (75% at 7 weeks) compared to other lines with impressive migration of up to 6 mm from the site of injection. At 12 weeks post-transplantation of the ciPS cells, cell survival was quantified at 275%, indicating the ciPS cells were continuing to proliferate and migrate. Indeed, staining for the proliferation marker Ki67 revealed that 19% of the HuNA+ cells were proliferating at 7 weeks post-transplantation. By 12 weeks, many of the HuNA+ cells stopped dividing with only 6% expressing Ki67.

We have identified these cells as possible candidates for the neuroprotection strategy of transplantation into SOD1 rats.

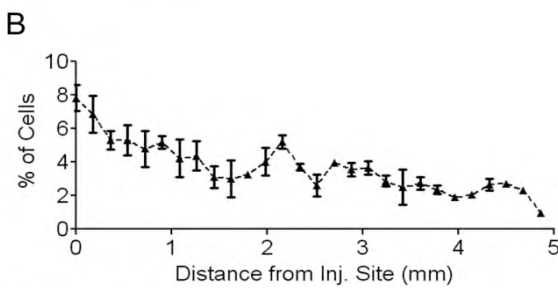
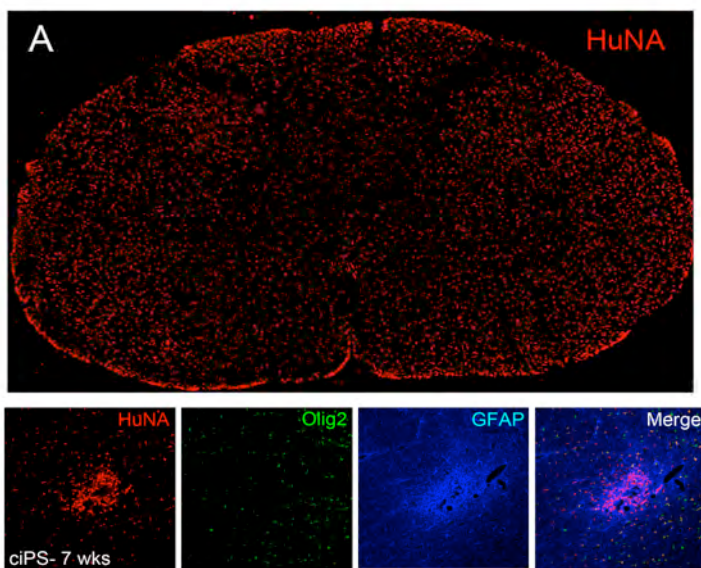


Figure 7

Figure 7. In rats receiving ciPS astrocyte transplants, HuNA+ cells could be localized after 12 weeks throughout the entire grey and white matter of the spinal cord (**A**). The HuNA+ ciPS cells were distributed evenly throughout the spinal cord instead of clustered at the injection site and in some sections, comprised over 50% of the DAPI+ cells in the spinal cord. Cells migrated several millimeters from transplantation site (**B**)

Significance: Most of the iPSC-glial progenitor cell lines studied have significant limitations for transplantation strategies with regard to cell survival and migration. These limitations are significantly different from the survival and distribution we have previously demonstrated in our utilization of human fetally-derived glial progenitor cells (Lepore et al 2011). However, we have identified a line of control iPSC-derived glial progenitor cells (the ci-IPS line) that seems to have better characteristics for our transplantation studies in ALS rats.

KEY RESEARCH ACCOMPLISHMENTS:

--Induced Pluripotent Stem Cell lines have been created from subjects with familial ALS, Sporadic ALS, and controls
--iPS Cell-derived astrocyte progenitors have been successfully developed from subjects with familial ALS, Sporadic ALS, and controls
--Initial transplantation experiments of iPS Cell-derived glial progenitors suggest that there is some variability among control iPS cell-derived lines with regard to survival, migration, and differentiation.
--Following transplantation, iPSC-derived glial progenitors continue to differentiate and develop more mature markers of astrocyte and oligodendrocyte identity.
--We have not yet appreciated any significant differences in the in vivo characterization of ALS iPSC-derived astroglial progenitors when compared with control astroglial progenitors.
--The complete characterization of the human iPSC-derived glial progenitors titled: "Gene profiling of human iPSC-derived astrocyte progenitors following spinal cord engraftment" has been submitted and is currently in revision. This manuscript examines iPSC-derived glial progenitor lines in spinal cords of control rats with regard to their survival, migration, differentiation, and gene expression profile.
--A second manuscript comparing the in vitro properties of human iPSC-derived glial progenitors from control and SOD1 subjects is in preparation tentatively titled: "A Comprehensive Library of Familial Human Amyotrophic Lateral Sclerosis Induced Pluripotent Stem Cells" in collaboration with Eggan, Henderson, and Rothstein.

REPORTABLE OUTCOMES: NONE

CONCLUSION:

This effort has resulted in several important advances. We have now developed an extensive library of fibroblasts and iPSCs from patients with sporadic ALS, familial ALS, and control subjects. We have been able to use these cells not just for our own purposes but also as part of numerous collaborations with other investigators worldwide. We have also rigorously analyzed the characteristics of both ALS and control iPSC-derived astrocyte progenitors in vitro to demonstrate (at least in the lines studied to date) that the baseline characteristics are similar. We have extended these observations to in vivo transplantation into rat spinal cords. Somewhat disappointingly, of the several control and single familial ALS lines studied, the survival and migration pattern of these cells was less than anticipated, and hoped, for widespread use as a therapeutic. However, one line with unique features (c-iPS) was identified with more impressive patterns of survival and migration following in vivo transplantation. This cell line that we have been using is likely the most appropriate for our future completion of therapeutic preclinical ALS transplantation studies.

REFERENCES: NONE

APPENDICES: "Gene profiling of human iPSC-derived astrocyte progenitors following spinal cord engraftment"

Gene profiling of human iPSC-derived astrocyte progenitors following spinal cord engraftment

Amanda M. Haidet-Phillips^a, Laurent Roybon^b, Sarah K. Gross^a, Alisha Tuteja^a, Christopher J. Donnelly^a, Myungsung Ko^a, Alex Sherman^a, Kevin Eggan^c, Christopher E. Henderson^b, Nicholas J. Maragakis^{a*}

^aDepartment of Neurology, Johns Hopkins University School of Medicine, Rangos 248, 855 North Wolfe Street, Baltimore, MD 21205.

^bDepartments of Pathology, Neurology, and Neuroscience, Center for Motor Neuron Biology and Disease, Columbia University Medical Center, Hammer Health Sciences Building, 701 West 168th Street, New York, NY 10032.

^cThe Howard Hughes Medical Institute, Harvard Stem Cell Institute and the Department of Stem Cell and Regenerative Biology, Harvard University, 7 Divinity Avenue, Cambridge, MA 02138.

* To whom correspondence should be addressed:

Nicholas J. Maragakis, M.D., Department of Neurology, The Johns Hopkins University School of Medicine, John G. Rangos Building, 855 North Wolfe Street, Room 248, Baltimore, MD 21205, Phone: 410-614-9874, Fax: 410-502-5459, E-mail: nmaragak@jhmi.edu

Running Head (<50 characters): Transplantation of hiPSC astrocyte progenitors

Author contributions: A.H.P.: conception and design, collection and/or assembly of data, data analysis and interpretation, manuscript writing, final approval of manuscript. L.R.: conception and design, data analysis and interpretation, manuscript writing. S.K.G., A.T., M.K., A.S.:

Collection and/or assembly of data. C.J.D.: conception and design, collection and/or assembly of data, data analysis and interpretation. K.E.: provision of study materials, final approval of manuscript. C.E.H.: provision of study materials, final approval of manuscript. N.J.M.: conception and design, data analysis and interpretation, manuscript writing, final approval of manuscript, financial support.

Acknowledgements: This work was supported by the ALS Association (fellowship to A.H.), The Michael S. and Karen G. Ansari ALS Center for Cell Therapy and Regeneration Research (N.J.M), The Department of Defense ALS Research Program (N.J.M.), The Maryland Stem Cell Research Foundation (N.J.M.), and P²ALS (N.J.M.).

Key Words: Human induced pluripotent stem cells, stem cell transplantation, astrocytes, gene profiling

Abstract (<250 words)

The generation of human induced pluripotent stem cells (hiPSCs) represents an exciting advancement with promise for stem cell transplantation therapies as well as for neurological disease modeling. Based on the emerging roles for astrocytes in neurological disorders, we investigated whether hiPSC-derived astrocyte progenitors could be engrafted to the rodent spinal cord and how the characteristics of these cells changed between *in vitro* culture and after transplantation to the *in vivo* spinal cord environment. Our results show that human embryonic stem cell (hESC)- and hiPSC-derived astrocyte progenitors survive long-term after spinal cord engraftment and differentiate to astrocytes *in vivo* with few cells from other lineages present. Gene profiling of the transplanted cells demonstrates the astrocyte progenitors continue to mature *in vivo* and upregulate a variety of astrocyte-specific genes. Given this mature astrocyte gene profile, this work highlights hiPSCs as a tool to investigate disease-related astrocyte biology using *in vivo* disease modeling with significant implications for human neurological diseases currently lacking animal models.

Body (<5000 words excluding references and figure legends)

Introduction

Stem cell transplantation strategies hold considerable promise in the understanding and treatment of a variety of neurological disorders. The *in vitro* use of neural stem cells has already gained traction as a platform for recreating the sequences of neural development, modeling disease phenotypes, and for potential use in drug screening against target-disease pathways. However, the correlation between the *in vitro* characteristics of these cells for those tasks and the *in vivo* characteristics of those same cells for therapeutic transplantation studies as well as more complex *in vivo* disease modeling has only had limited investigation.

Various stem cell sources have been evaluated for brain and/or spinal cord engraftment studies including human embryonic stem cells (hESCs), mesenchymal stem cells, fatally-

derived neural stem cells, and more recently human induced pluripotent stem cells (hiPSCs).¹⁻⁴ Human iPSCs were initially reprogrammed from adult human fibroblasts and have been shown to be capable of differentiating into neural-specific cell lineages.⁵ Enthusiasm for the potential of hiPSCs in treating neurological disorders has also grown, especially for diseases involving damaged or diseased glia including spinal cord injury, multiple sclerosis, and other demyelinating disorders.^{1, 6} The discovery that hiPSC-derived oligodendrocyte progenitors can extensively remyelinate and rescue a mouse model of congenital hypomyelination has generated promise for both adult demyelinating and degenerative disorders as well as infantile oligodendroglial disorders.⁷ Indeed, the first clinical trial involving transplantation of hESC-derived oligodendrocyte progenitors into patients with spinal cord injury was approved in 2009, paving the way for future trials involving the use of hiPSCs. Since then, a second trial testing transplantation of hESC-derived retinal pigment epithelium for macular degeneration has importantly reported no safety concerns involving the use of these cells.⁸

In addition to their promise as a cellular source for transplantation therapies, hiPSCs can also be utilized as valuable tools in the modeling of human disease.^{9, 10} The generation of hiPSCs from living patients may be especially useful for neurological diseases for which diseased patient tissue is inaccessible through biopsy. Human iPSCs have already been generated from patients with a large variety of neurological disorders, and after differentiation toward neural cell fates, these hiPSCs have excitingly displayed diseased-related phenotypes *in vitro* for a number of diseases.^{9, 10}

While the majority of hiPSC work has focused on the production of neurons or oligodendrocytes from hiPSCs, it has become evident that astrocytes also play critical roles in both the healthy nervous system as well as in various conditions, notably Amyotrophic Lateral Sclerosis (ALS), Rett's Syndrome, and Huntington's Disease.^{11, 12} Specifically, astrocytes expressing disease-linked mutant genes have been shown to directly cause neurotoxicity in these diseases. Since astrocytes are either damaged or pathologically altered in these

disorders, transplantation of healthy astrocytes may limit neurotoxicity and provide additional support to injured neurons. In addition to the therapeutic goals of stem cell transplantation, generation and transplantation of patient hiPSC-derived astrocytes may be useful for *in vivo* disease modeling. This is especially true for diseases such as sporadic ALS, where a genetic component has not been identified as the etiology in the majority of cases. Therefore, disease modeling by transplantation of patient-derived hiPSCs into the spinal cord may currently be one of the best means to study cell-specific disease mechanisms *in vivo*.

The goal of our study was to develop a transplantation paradigm for the engraftment of hiPSC-derived astrocytes for disease modeling purposes as well as to evaluate the potential of these cells as a source for therapeutic transplantation. Since transplantation of hiPSC-derived neural stem cells yields mainly neurons or a mixture of neural cell types,¹³⁻¹⁵ we aimed to first differentiate hiPSCs into astrocyte progenitors *in vitro* and then evaluate their capacity to survive and engraft when transplanted into the ventral horn of the adult rodent spinal cord. In addition, a critical question to the stem cell transplantation field is whether progenitor cells continue to differentiate after transplantation and adopt mature properties *in vivo* which may be essential for their potential therapeutic benefits in patients. In evaluation of the hiPSC-derived astrocyte progenitors, we utilized a novel human-specific gene profiling approach to compare the *in vivo* expression profile between various stem cell lines after transplantation to the spinal cord. We also employed this gene profiling approach to compare the expression profiles of the astrocyte progenitors *in vitro* versus the expression profile after engraftment to evaluate how these cells mature in an *in vivo* environment.

Our data show that both hESC- and hiPSC-derived astrocyte progenitors are capable of engrafting and surviving in the rat spinal cord for at least 12 weeks. Immunohistochemical analysis and gene profiling of the transplanted human cells revealed the astrocyte progenitors efficiently differentiate into astrocytes *in vivo* with few cells from other neural lineages present. Additionally, gene profiling of the transplanted human cells shows that the astrocyte progenitors

mature dramatically *in vivo* after transplantation and upregulate a variety of both structural and functional astrocyte genes. This observed maturation highlights their potential for use for *in vivo* disease modeling using patient-derived hiPSCs to study diseases of the brain and spinal cord.

Materials and Methods

iPSC generation and characterization. Retroviruses expressing Sox2, Oct4, and Klf4 were used to reprogram fibroblasts to create the 11a and 18c iPSC lines. The characterization of these iPSC lines has been previously described¹⁶. Briefly, these iPSC lines were evaluated for expression of the pluripotency factors alkaline phosphatase, NANOG, OCT4, SSEA3, SSEA4, TRA-1-60, and TRA-1-81. All iPSC lines were also analyzed for the ability to form three germ layers in an *in vitro* assay as well as the ability to form teratomas after transplantation into immune compromised mice. Details describing differentiation of hiPSCs are provided in Supporting Information.

Rats: Sprague-Dawley rats (9-10 weeks old, Taconic) were dosed daily with cyclosporine (20 mg/kg, Novartis) by subcutaneous injection beginning 3 days prior to transplantation and continued until sacrifice. The care and treatment of animals in all procedures was conducted in strict accordance with the guidelines set by the NIH Guide for the Care and Use of Laboratory Animals, the Guidelines for the Use of Animals in Neuroscience Research and the Johns Hopkins University IACUC, and measures were taken to minimize any potential pain or animal discomfort.

Transplants: Rats were anaesthetized and cervical laminectomy performed. Each rat received bilateral injections into the ventral horn at the 6th cervical spinal level (C6) for a total of 2 injections. Each injection contained 150,000 cells in a total of 2 µl delivered using a 10 µl Hamilton syringe secured to a micromanipulator with microsyringe pump controller (1 µl/minute rate).¹⁷

Nanostring® Analysis: Rats were perfused with 0.9% saline and spinal cord tissue was harvested and fast-frozen in liquid nitrogen. RNA was isolated using Trizol, followed by DNase

treatment and RNA cleanup using RNAeasy columns (Qiagen). As a control, RNA was also isolated using identical methods from three control human cervical spinal cords. See Supporting Information Table S1 for probe sequence and target genes used. For the Nanostring® assay, 100 ng of RNA was loaded per sample. For analyses comparing gene expression of transplanted cells across the spinal cord (Fig. 4 and Supporting Information Table S2) as well as analysis of human spinal cord (Supporting Information Fig. S5), all samples were normalized using internal positive controls and the raw total counts after normalization were graphed. For analyses comparing gene expression between cell lines *in vitro* as well as analyses comparing gene expression *in vitro* versus *in vivo* (Fig. 5, Fig. 6, Supporting Information Fig. S6, Supporting Information Table S3, Supporting Information Table S4), all samples were normalized using internal positive controls and 4 human specific housekeeping genes (B2M, GAPDH, GUSB, OAZ1) and total counts after normalization were graphed. Prior to normalization, all raw values reading less than 10 total counts were eliminated from analysis since they were under the standard limit of detection.

Statistical Analysis: All data were analyzed using Graph Pad Prism software. Data in all graphs are represented as the mean +/- SEM and were analyzed using one-way ANOVA. For immunohistochemistry analysis, we analyzed at least 3 injection sites for *in vivo* analysis and at least 3 wells for *in vitro* cultures. For transplantation studies, number of animals used is represented for each cell line in Table 1 and two independent transplant sites were analyzed for all rats.

Results

Directed differentiation of hESCs and hiPSCs to astrocyte progenitors

To assess astrocyte engraftment potential from hiPSCs and hESCs, we utilized 2 hiPSC lines created from healthy individuals as well as one hESC line for *in vitro* astrocyte progenitor generation (Table 1). All hiPSC and hESC lines had a normal karyotype, expressed pluripotency markers, and were capable of differentiating to all three embryonic germ layers.^{16, 18} Astrocytes

were generated from hESCs and hiPSCs using previously characterized protocols (Roybon et al, In press). Briefly, hiPSCs and hESCs were neuralized with BMP4 and Activin/TGF- β antagonists, followed by caudalization and ventralization using retinoic acid and sonic hedgehog, respectively (Fig. 1A). By day 15 of differentiation, neural stem cells were identifiable by Pax6/Sox2/Nestin staining and were differentiated to glia using media supplementation with 1% FBS. Astrocyte precursors as defined by CD44 staining were usually noticed by day 50-60 of differentiation and after 100 days, between 30-50% of cells were expressing GFAP depending on the cell line (Fig. 1B, C).¹⁹ No Olig2 $^+$ oligodendrocyte lineage cells were observed in the cultures and rare (<1%) Tuj1 $^+$ neurons could be identified. However, the majority of cells still expressed Nestin as well as CD44 at the end of the differentiation process, indicating the culture was a mixture of astrocyte progenitor cells and immature GFAP $^+$ astrocytes.

Transplantation of hESC- and hiPSC-derived astrocyte progenitors to the rat spinal cord

To evaluate the astrocyte progenitors' propensity for engraftment, the cells were transplanted bilaterally to the ventral horn of the cervical spinal cord of adult wild-type rats. Prior to the injection and for the remainder of the study, rats were given high-dose cyclosporine to prevent immune rejection of the grafted human cells. Rats were sacrificed at 2, 7, or 12 weeks post-transplantation (Table 1). All rats were observed daily and no behavioral abnormalities were noted for the entirety of the study. At 2 weeks post-transplantation, cells could be localized in the spinal cord by staining for human-specific nuclear antigen (HuNA) and most of the transplanted cells resided within 1 mm rostral-caudal from the transplantation site (Supporting Information Fig. S1). Evaluation of the transplanted cells at 7 weeks (Supporting Information Fig. S2) and 12 weeks (Fig. 2 A-D) post-transplantation revealed the HuNA $^+$ cells could be localized in the spinal cord at these time points with limited (< 1 mm) rostral-caudal migration from the transplantation site. Quantification of HuNA $^+$ cells in the spinal cord at 2, 7, and 12 weeks post-transplantation showed that the transplanted cells survived for up to 12 weeks (Fig. 2E) with the majority of cells residing in the grey matter of the spinal cord (Fig. 2F). No large

differences in the survival and migration were noted between the different lines of hESCs and hiPSCs after transplantation at any of the time points examined. Additionally, no teratoma formation was noted in any of the rats at any time point examined.

Cell lineage characterization of transplanted hESC- and hiPSC-derived astrocyte progenitors

To determine whether the transplanted cells retained their astrocyte lineage after engraftment, we co-localized HuNA⁺ cells with various cell lineage markers to assess whether the human cells differentiated into GFAP⁺ astrocytes, Tuj1⁺ neurons, or Olig2⁺ cells of the oligodendrocyte lineage. At the time of transplantation, the majority of the differentiated cells expressed Nestin and CD44 *in vitro* with 30-50% of these cells expressing GFAP depending on the cell line (Fig. 1C). However, after transplantation of the hiPSC lines and the hESC line, over 80% of the transplanted HuNA⁺ cells expressed GFAP at 2 weeks post-transplantation (Fig. 3A). Immunohistochemical analysis of the transplanted cells at 7 weeks (Supporting Information Fig. S3A) and 12 weeks (Fig. 3B, C) post-transplantation showed that over 90% of the HuNA⁺ cells express GFAP at these time points, suggesting the majority of transplanted astrocyte progenitors differentiate within 2 weeks to GFAP⁺ astrocytes and remain stable for at least 12 weeks. To verify the localization of the nuclear HuNA antigen with cytoplasmic markers such as GFAP, we also utilized an antibody specific for human mitochondria (hMito) which co-localized with GFAP (Fig. 3D). Additionally, the transplanted cells could be localized using a human-specific GFAP antibody which allowed us to observe their elaborate morphologies *in vivo* (Fig. 3E). The HuNA⁺ transplanted cells also expressed the astrocytic water channel, aquaporin 4, consistent with a mature astrocyte profile of gene expression (Fig. 3F). Few HuNA⁺/Olig2⁺ cells were noted (Fig. 3G) and no HuNA⁺Tuj1⁺ cells were observed in these lines although transplanted cells resided close in proximity to endogenous rat neurons (Supporting Information Fig. S3B). Overall, the astrocyte progenitors derived from different hESC and hiPSC lines did not significantly differ in their differentiation profile post-transplantation. Since only a fraction of the cells from the hESC and hiPSC lines expressed GFAP at the time of transplantation, these

data suggest that the GFAP⁻/CD44⁺ fraction of cells differentiated *in vivo* to GFAP⁺ astrocytes within 2 weeks of transplantation. Another possibility is that the increase in GFAP reactivity indicates transition to a reactive astrocyte phenotype after transplantation. Therefore, we evaluated the transplanted cells for expression of LCN2, a recently identified marker for reactive astrocytes.²⁰⁻²² Although we could detect LCN2 in the spinal cord ventral horn of human ALS patients, we observed no LCN2 expression from HuNA⁺ transplanted cells, suggesting the transplanted astrocyte progenitors did not differentiate to a reactive phenotype *in vivo* (Supporting Information Fig. S4).

In vivo gene profiling of transplanted hESC- and hiPSC-derived astrocyte progenitors

To more fully characterize the phenotype of the transplanted human cells, we sought to develop a gene profiling system to evaluate *in vivo* human-specific gene expression since there exists limited human-specific antibodies appropriate for IHC analysis of astrocytes. For these studies, we utilized Nanostring® technology which is a probe-based method for direct RNA quantification that allows for both sensitive and specific detection of small amounts of human-specific RNAs without cDNA conversion or further amplification steps.²³ We designed a custom panel of over 50 genes (Supporting Information Table S1) including well described genes expressed by neural progenitor cells, neurons, oligodendrocytes, and astrocytes as well as less characterized genes found to be expressed specifically in astrocytes *in vivo* by gene profiling methods.²⁴ The design of human-specific RNA probes allows for measurement of gene expression levels specifically in the transplanted human cells within the rat spinal cord to create a gene expression profile for the engrafted human astrocyte progenitors.

For each line of transplanted hESC or hiPSC-derived astrocyte progenitors, we analyzed *in vivo* gene expression at 12 weeks post-transplantation. We isolated RNA for gene expression profiling from the cervical spinal cord region at the injection site, from cervical sections rostral and caudal to the injection site, as well as from a lumbar section of the spinal cord, a remote site from the area of transplant. Since we observe few transplant-derived cells migrating even into

the thoracic region of the spinal cord, we chose the lumbar region as an area where no human RNAs are present. The lumbar region was used to evaluate for any background cross reactivity of the human-specific probes with endogenous rat RNAs.

Analysis of *in vivo* gene expression of transplanted astrocyte progenitors from the hiPSC and hESC lines showed that the transplanted cells expressed a wide array of astrocyte lineage genes *in vivo* (Fig. 4 A-C, Supporting Information Table S2). These genes included structural astrocyte genes such as GFAP as well as functional genes expressed by mature *in vivo* astrocytes such as the water channel, Aquaporin 4, the gap-junction protein, Connexin 43, the membrane-associated protein, MLC1, the glutamate transporters, EAAT1, and to a lesser extent EAAT2 in some cell lines. For many of the astrocyte lineage genes, expression was highest at the transplant site and then decreased in a gradient fashion rostral and caudal from the transplant site (Fig. 4 A-C). We also evaluated human gene expression in three control post-mortem human spinal cords and found a similar pattern of astrocyte gene expression, including high GFAP expression with lower but detectable expression of other astrocyte lineage genes such as Aquaporin 4 and glutamate transporters (Supporting Information Fig S5).

Although we could detect high expression levels of a variety of astrocyte-specific genes, we did not detect any neuronal-specific genes (NeuroD, β -tubulin) expressed by the transplanted cells (Fig. 4 D-F), consistent with the immunohistochemical results showing the transplanted cells do not differentiate into neurons *in vivo* (Fig. 3B). Similarly, no transplant-derived expression of microglial-specific genes (ITGAM) was found (Fig. 4 D-F). However, we were able to detect human-specific transcripts for progenitor cell markers such as Nestin and Sox2, indicating some of the transplanted cells may reside in an immature progenitor state *in vivo* (Fig. 4 D-F). Likewise, we could also detect low levels of expression of early oligodendrocyte lineage genes such as Olig2, PDGFR- α , and CNP which is consistent with the immunohistochemical analysis showing that a small percent (<5%) of cells differentiate toward the oligodendrocyte lineage *in vivo*. Mature oligodendrocyte genes related to myelin production

such as MOG were not expressed by the transplanted cells at 12 weeks post-transplantation (Fig. 4 D-F). Overall, we did not notice large differences between the lines (H13, 11a, and 18c) in their *in vivo* gene profile after transplantation. The only noted difference was that the total level of astrocyte gene expression was lower in the 11a line compared to the 18c and H13 lines (Fig. 4 A-C). These results could indicate the 11a line did not mature as well into astrocytes as the other 2 cell lines. More likely though, these results reflect the low survival of this cell line after transplantation (Fig. 2E) with fewer cells surviving corresponding to fewer human astrocyte transcripts detected overall in the spinal cord.

Gene profiling reveals maturation of hESC- and hiPSC-derived astrocyte progenitors post-transplantation

In addition to characterizing the *in vivo* gene expression profile of the transplanted cells, we furthermore asked how the gene expression profile of these cells compared to their expression profile *in vitro* just prior to transplant. For therapeutic transplantation purposes, it is crucial to know whether engrafted cells continue to differentiate *in vivo* and adopt the properties of mature astrocytes or whether they reside in an immature state after transplantation. Immunohistochemical analysis of the differentiated hESCs and hiPSCs *in vitro* showed that these cells express markers indicative of an astrocyte progenitor phenotype prior to transplant (GFAP, CD44, Nestin) (Fig. 1C). *In vitro* gene profiling of the astrocyte progenitors prior to transplant also indicates these cells express both immature stem cell markers such as Nestin, Sox2, and CD44 as well as some astrocyte lineage genes such as GFAP, Connexin 43, and EAAT1 (Supporting Information Fig. S6 A-B, Table S3). These gene profiling results are consistent with the immunohistochemical data (Fig. 1C) indicating the highest level of GFAP expression in the H13 line, followed by the 18c line, and then the 11a line with the lowest GFAP expression level prior to transplant (Supporting Information Fig. S6A).

We sought to determine whether the expression of these astrocyte lineage genes increases after transplantation and whether the transplanted cells begin to express a more

mature profile of astrocyte lineage genes after transplant. To compare the *in vitro* gene expression profile with the post-transplant gene expression profile, we normalized using human-specific housekeeping genes to specifically compare the level of human-specific gene expression *in vitro* versus *in vivo*. Using this method, we found that astrocyte-specific gene expression within the transplanted cells increased dramatically (note log scale on graphs) after engraftment to the rat spinal cord (Fig. 5, Supporting Information Table S4). Structural genes such as GFAP were upregulated 100-500 fold (depending on the cell line) after transplantation and some functional genes such as EAAT1 and EAAT2 were upregulated between 30-500 fold in most of the human cell lines *in vivo*. Of the top 20 astrocyte-specific genes found in a previous gene profiling report of *in vivo* astrocytes,²⁴ about half of these genes were increased after transplant in the 11a, 18c, and H13 lines (Fig. 5). Again, we noticed no striking differences in cell maturation between the different lines after transplant although fewer astrocyte-specific genes were above the limit of detection in the 11a line (Fig. 5B).

In addition to examining whether astrocyte-specific genes increase after transplantation, we also analyzed the expression of a variety of genes which have been shown from mouse gene profiling studies to increase or decrease as astrocytes mature from P7 to P17 *in vivo*.²⁴ We were interested to know whether our human stem cell-derived astrocyte progenitors expressed these genes prior to transplantation and whether they were upregulated after transplantation. In addition, we also analyzed expression of genes shown to be enriched in cultured mouse astrocytes compared to *in vivo* mouse astrocytes²⁴ to determine whether these genes are expressed in our cell lines *in vitro* and if so, whether they are downregulated after transplantation.

In general, we saw that all of our hESC- and hiPSC-derived astrocyte progenitors prior to transplantation express a variety of genes previously shown to be enriched in *in vitro* cultured astrocytes (Fig. 6). However, after transplantation, all of these genes with the exception of Anxa1 were downregulated to undetectable levels within the human cells, indicating a

phenotypic maturation post-transplantation (Fig. 6). Furthermore, a variety of genes specifically enriched in developing astrocytes (P7) compared to mature astrocytes (P17) were also expressed in the hESC- and hiPSC-derived astrocyte progenitors prior to transplant (Fig. 6). Similar to the expression profile for *in vitro* culture-related genes, after transplantation, we observed a general downregulation of these genes in the human cells, and in two of the transplanted cell lines (11a and 18c) we could not even detect many of these development-related genes *in vivo* (Fig. 6). In contrast, when we analyzed genes enriched in mature mouse astrocytes (P17) compared to P7 mouse astrocytes, we observed no clear pattern of up or down regulation after transplant (Fig. 6). These observations may mean that the engrafted astrocytes are not yet fully mature, although their expression of other mature astrocyte-specific genes indicates otherwise. Alternatively, these observations may reflect differences in the development of mouse compared to human astrocytes *in vivo* as well as the observation that the mouse astrocyte genes were profiled from a forebrain population which may not be a general representation of all astrocytes.

Discussion

One of the most significant advances in the stem cell biology field has been the generation of hiPSCs and development of protocols allowing differentiation of hiPSCs to specific cell lineages. Human iPSCs are promising for autologous cell transplantation therapies since they can be generated from a living patient and theoretically, transplanted back into the same patient without concern of immune-mediated rejection based on genetic variations between the cells and the recipient. In addition, hiPSCs can be derived from patients with neurological disorders for disease modeling purposes which may lead to further understanding of diseases for which genetic contributors are unknown or reliable mouse models are not available.

Based on the increasingly important role for glia in neurodegenerative disorders, we focused on hiPSC-derived astrocyte progenitors and transplantation of these cells to the spinal cord. Astrocytes expressing mutant disease-linked genes have been shown to directly

contribute to neurotoxicity in ALS as well as in other diseases such as Rett's Syndrome.^{11, 12} Thus, replacement of the aberrant astrocyte population in the spinal cord may be neuroprotective in ALS and other disorders. Additionally, for the majority of ALS patients, there is no known genetic contributor to the development of the disease (sporadic ALS). This presents difficulties in the study of basic disease-related mechanisms. *In vivo* disease modeling through engraftment of patient-derived hiPSCs to the rodent spinal cord may be one means to study astrocytes from these sporadic ALS patients in an *in vivo* environment. *In vivo* disease modeling strategies have been attempted by transplantation of patient hiPSC-derived neurons for Huntington's disease,²⁵ but similar measures using patient hiPSC-derived glia (rather than neurons) have not been attempted for ALS or other neurodegenerative diseases.

In this work, we investigated the propensity for engraftment of astrocyte progenitors derived from both hESC and hiPSC lines from healthy individuals as a first step towards characterizing these cells both *in vitro* and *in vivo*. Our data show that these astrocyte progenitors are capable of engrafting into the spinal cord and surviving long-term (at least 12 weeks) after transplantation. Although only a proportion of the cells expressed GFAP *in vitro*, post-transplantation, over 90% of the cells expressed GFAP, indicating the astrocyte progenitors matured into astrocytes *in vivo* with very few cells of other lineages present. Further gene profiling at 12 weeks post-transplantation indicated the transplanted cells express a gene profile consistent with mature astrocytes *in vivo* including upregulation of many astrocyte-specific genes after transplant.

One challenge we encountered in transplantation of the astrocyte progenitors was their limited survival and migration after transplant. Transplantation of less differentiated human fetal-derived and hiPSC-derived glial precursor cells results in much improved survival and migration, most likely a consequence of their proliferative capacity *in vivo* after transplant.^{7, 26, 27} However, glial precursors have the ability to differentiate into astrocytes or oligodendrocytes and this split differentiation profile was observed after transplantation of both fetal-derived and hiPSC-derived

cells.^{7, 26, 27} The resulting mixture of astrocytes and oligodendrocytes after transplant may present challenges in analyzing the specific contributions of astrocytes or oligodendrocytes in the context of *in vivo* disease modeling. In contrast, in the current study, we observed over 90% of the hESC- and hiPSC-derived astrocyte progenitors differentiating into astrocytes *in vivo*. Therefore, transplantation of hiPSC-derived astrocyte progenitors may be more suitable for *in vivo* modeling of focal astrocyte-specific influences on spinal motor neurons in diseases such as ALS. Improvement in survival and migration of the astrocyte progenitors while retaining a restricted cell fate continues to present a challenge in using these cells for therapeutic purposes. Only one other study has described attempted transplantation of hESC-derived astrocyte progenitors; however, this study did not provide any quantitative data on the survival, migration, or differentiation profile of these cells *in vivo* and these transplantation studies were also limited to hESC-derived astrocyte progenitors (not hiPSCs).²⁸

Due to the limited availability of human-specific antibodies, we tested a novel method to assess human-specific gene expression *in vivo* after transplantation using Nanostring® gene profiling. This gene profiling approach allows for rapid assessment of *in vivo* gene expression using customizable human-specific probes, providing a snap-shot of how the transplanted cells behave *in vivo* after transplantation. Using this method, we were able to show that the transplanted astrocytes express a wide array of astrocyte-specific genes *in vivo*, which would have been challenging by standard immunohistochemical measures.

Another goal of our work was to use gene profiling to assess how the transplanted cells change between *in vitro* culture versus after transplantation to the *in vivo* environment of the rodent spinal cord. Transcriptome analyses indicate a clear difference between astrocytes cultured *in vitro* versus *in vivo* endogenous astrocytes of the rodent forebrain.²⁴ Many of the perceived benefits of engrafted astrocytes rely on mature functions of these cells which may or may not be present in the transplanted cells. For example, in ALS, astrocytes are well known to lose expression of the major glial glutamate transporter, EAAT2, causing excess glutamate to

accumulate at the synapse and downstream neurotoxicity.²⁹⁻³¹ Our data show that the transplanted astrocyte progenitors express a variety of both structural (GFAP) and functional genes such as the water channel, aquaporin 4, the gap junction protein, connexin 43, and glutamate transporters. Additionally, gene profiling demonstrates that the transplanted cells undergo significant maturation after engraftment leading to upregulation of a variety of astrocyte-specific genes and downregulation of genes involved in astrocyte development. Since we only measured the gene profile of the transplanted cells out to 12 weeks post-transplantation, the possibility also exists that these cells will continue to mature and express even higher levels of mature astrocyte genes at later time points *in vivo*. Still, these data highlight the potential usefulness for hiPSCs in *in vivo* modeling for diseases such as ALS where astrocytes have been implicated in disease initiation and progression.

Lastly, while our understanding of hiPSCs has grown dramatically in recent years, much of this work has been limited to *in vitro* studies. Several *in vitro* studies have suggested that hESCs differ significantly from hiPSCs and have also highlighted substantial variation between different lines of hiPSCs in gene expression and differentiation potential.^{16, 32-38} We asked whether these variations exist only *in vitro* or whether cell line-specific differences are also present after transplantation to the spinal cord. In our work, all 3 cell lines we transplanted behaved similarly *in vivo* with regard to survival, migration, and differentiation. We also noted no large differences between the hESC line and the 2 iPSC lines before or after transplant. While our data include only 3 different cell lines, Nanostring® gene profiling may provide for a way to more quickly screen further cell lines to assess for line variability in survival, migration, and differentiation *in vivo*.

Conclusions

In conclusion, we have evaluated hiPSC- and hESC-derived astrocyte progenitors for their ability to engraft into the rodent spinal cord as the first step toward cell transplantation therapy and *in vivo* disease modeling using these cells. Although migration and initial survival

was limited after transplantation of these cells, we did observe restricted differentiation to astrocytes *in vivo* with few cells from other lineages present. Our novel gene profiling approach showed that hESC- and hiPSC-derived astrocyte progenitors continue to develop *in vivo* after transplantation and express mature astrocyte genes suggesting the cells received *in vivo* environmental cues directing them toward terminal differentiation. Given the homogenous differentiation profile and mature gene expression of these cells, transplantation of patient-derived hiPSC astrocyte progenitors for *in vivo* disease modeling or for potential therapeutics in the spinal cord is feasible. Establishment of hiPSC-derived astrocyte progenitors as a tool for *in vivo* disease modeling may then lead to the discovery of novel mechanisms in ALS or other neurodegenerative disorders with astrocyte dysfunction.

Figure Legends

Fig. 1. *In vitro* differentiation of hESCs and hiPSCs into astrocyte progenitors. **(A)** Timeline for differentiation into astrocyte progenitors prior to transplantation. **(B, C)** At the time of transplantation, the differentiated cells of all cell lines express markers indicative of an astrocyte progenitor phenotype. Not detected, N.D. Scale bars=10 μ m.

Fig. 2. Characterization of hESC- and hiPSC-derived astrocyte progenitors after transplantation to the rat spinal cord. **(A-C)** Human ESC- (A) and iPSC- (B-C) derived astrocyte progenitors can be localized by human nuclear antigen (HuNA) at 12 weeks post-transplantation and many express GFAP *in vivo*. Scale bars=50 μ m. **(D)** Rostral-caudal cell migration from the site of injection (inj.) was measured at 12 weeks post-transplantation by calculating the percent of total HuNA $^{+}$ cells along the distance of the spinal cord. **(E)** Cell survival at 2, 7, and 12 weeks post-transplantation was quantified by counting HuNA $^{+}$ transplanted cells throughout the spinal cord. **(F)** Grey matter (GM)/white matter (WM) localization of transplanted HuNA $^{+}$ cells was assessed at 2, 7, and 12 weeks post-transplantation for all hESC and hiPSC lines.

Fig. 3. hESC- and hiPSC-derived astrocyte progenitors differentiate into astrocytes after transplantation to the rat spinal cord. **(A, B)** The percent of HuNA⁺ cells that also express GFAP, Olig2, or Tuj1 was quantified at 2 weeks (A) and 12 weeks (B) post-transplantation. Not detected, N.D. **(C)** Transplanted HuNA⁺ cells express GFAP and display typical astrocyte morphology. Scale bar=10 μ m. **(D)** Transplanted human cells show co-localization of human mitochondrial marker (hMito) and GFAP. Scale bar=10 μ m. **(E)** The transplanted cells can be recognized using a human-specific GFAP antibody (hGFAP) and elaborate complex morphologies *in vivo*. Scale bar = 100 μ m. The far right panel shows hGFAP expression magnified at high power. Scale bar = 10 μ m. **(F)** HuNA⁺ cells co-localizing with GFAP also express the astrocytic water channel, aquaporin 4 (Aq4). Scale bar = 10 μ m. **(G)** Few HuNA⁺ cells co-localize with the oligodendrocyte marker Olig2. Arrow denotes one HuNA⁺/Olig2⁺ cell. Scale bar = 10 μ m.

Fig. 4. Human-specific *in vivo* gene profiling of transplanted hESC- and hiPSC-derived astrocyte progenitors across cervical (C3-C7) and L1 lumbar segments of the spinal cord. **(A-C)** Gene profiling reveals expression of astrocyte lineage genes by transplanted H13 (A), 11a (B), and 18c (C) cells *in vivo*. **(D-E)** Gene profiling of non-astrocyte lineage genes expressed by transplanted H13 (D), 11a (E), and 18c (F) cells *in vivo*.

Fig. 5. Human-specific gene profiling of hESC- and hiPSC-derived astrocyte progenitors for astrocyte-specific genes *in vitro* prior to transplantation and *in vivo* after transplantation. **(A-C)** Gene profiling reveals increased expression of astrocyte-specific genes by H13 (A), 11a (B), and 18c (C) cell lines *in vivo* versus *in vitro*. The lack of a blue or yellow bar indicates that gene expression was below the limit of detection. Note: a logarithmic scale is used in all graphs of this figure.

Fig. 6. Human-specific gene profiling of hESC- and hiPSC-derived progenitors for genes involved in astrocyte development *in vitro* prior to transplantation and *in vivo* after transplantation. **(A-C)** Gene profiling reveals downregulation of many genes related to astrocyte

in vitro culture and early development after transplantation of H13 (A), 11a (B), 18c (C), and H13 (D) astrocyte progenitors to the spinal cord. The lack of a blue or yellow bar indicates that gene expression was below the limit of detection. Note: a logarithmic scale is used in all graphs of this figure.

References

1. Lukovic D, Moreno Manzano V, Stojkovic M, et al. Concise review: human pluripotent stem cells in the treatment of spinal cord injury. *Stem Cells*. 2012;30:1787-1792.
2. Papadeas ST, Maragakis NJ. Advances in stem cell research for Amyotrophic Lateral Sclerosis. *Curr Opin Biotechnol*. 2009;20:545-551.
3. Uccelli A, Laroni A, Freedman MS. Mesenchymal stem cells for the treatment of multiple sclerosis and other neurological diseases. *Lancet Neurol*. 2011;10:649-656.
4. De Feo D, Merlini A, Laterza C, et al. Neural stem cell transplantation in central nervous system disorders: from cell replacement to neuroprotection. *Curr Opin Neurol*. 2012;25:322-333.
5. Takahashi K, Tanabe K, Ohnuki M, et al. Induction of pluripotent stem cells from adult human fibroblasts by defined factors. *Cell*. 2007;131:861-872.
6. Goldman SA, Nedergaard M, Windrem MS. Glial progenitor cell-based treatment and modeling of neurological disease. *Science*. 2012;338:491-495.
7. Wang S, Bates J, Li X, et al. Human iPSC-derived oligodendrocyte progenitor cells can myelinate and rescue a mouse model of congenital hypomyelination. *Cell Stem Cell*. 2013;12:252-264.
8. Schwartz SD, Hubschman JP, Heilwell G, et al. Embryonic stem cell trials for macular degeneration: a preliminary report. *Lancet*. 2012;379:713-720.

9. Bellin M, Marchetto MC, Gage FH, et al. Induced pluripotent stem cells: the new patient? *Nat Rev Mol Cell Biol.* 2012;13:713-726.
10. Ito D, Okano H, Suzuki N. Accelerating progress in induced pluripotent stem cell research for neurological diseases. *Ann Neurol.* 2012;72:167-174.
11. Ilieva H, Polymenidou M, Cleveland DW. Non-cell autonomous toxicity in neurodegenerative disorders: ALS and beyond. *J Cell Biol.* 2009;187:761-772.
12. Molofsky AV, Krencik R, Ullian EM, et al. Astrocytes and disease: a neurodevelopmental perspective. *Genes Dev.* 2012;26:891-907.
13. Fujimoto Y, Abematsu M, Falk A, et al. Treatment of a mouse model of spinal cord injury by transplantation of human induced pluripotent stem cell-derived long-term self-renewing neuroepithelial-like stem cells. *Stem Cells.* 2012;30:1163-1173.
14. Major T, Menon J, Auyeung G, et al. Transgene excision has no impact on in vivo integration of human iPS derived neural precursors. *PLoS One.* 2011;6:e24687.
15. Nori S, Okada Y, Yasuda A, et al. Grafted human-induced pluripotent stem-cell-derived neurospheres promote motor functional recovery after spinal cord injury in mice. *Proc Natl Acad Sci U S A.* 2011;108:16825-16830.
16. Boulting GL, Kiskinis E, Croft GF, et al. A functionally characterized test set of human induced pluripotent stem cells. *Nat Biotechnol.* 2011;29:279-286.
17. Lepore AC, Rauck B, Dejea C, et al. Focal transplantation-based astrocyte replacement is neuroprotective in a model of motor neuron disease. *Nat Neurosci.* 2008;11:1294-1301.
18. Cowan CA, Klimanskaya I, McMahon J, et al. Derivation of embryonic stem-cell lines from human blastocysts. *N Engl J Med.* 2004;350:1353-1356.
19. Liu Y, Han SS, Wu Y, et al. CD44 expression identifies astrocyte-restricted precursor cells. *Dev Biol.* 2004;276:31-46.

20. Zamanian JL, Xu L, Foo LC, et al. Genomic analysis of reactive astrogliosis. *J Neurosci*. 2012;32:6391-6410.
21. Lee S, Park JY, Lee WH, et al. Lipocalin-2 is an autocrine mediator of reactive astrocytosis. *J Neurosci*. 2009;29:234-249.
22. Bi F, Huang C, Tong J, et al. Reactive astrocytes secrete lcn2 to promote neuron death. *Proc Natl Acad Sci U S A*. 2013;110:4069-4074.
23. Geiss GK, Bumgarner RE, Birditt B, et al. Direct multiplexed measurement of gene expression with color-coded probe pairs. *Nat Biotechnol*. 2008;26:317-325.
24. Cahoy JD, Emery B, Kaushal A, et al. A transcriptome database for astrocytes, neurons, and oligodendrocytes: a new resource for understanding brain development and function. *J Neurosci*. 2008;28:264-278.
25. Jeon I, Lee N, Li JY, et al. Neuronal properties, in vivo effects, and pathology of a Huntington's disease patient-derived induced pluripotent stem cells. *Stem Cells*. 2012;30:2054-2062.
26. Lepore AC, O'Donnell J, Kim AS, et al. Human glial-restricted progenitor transplantation into cervical spinal cord of the SOD1 mouse model of ALS. *PLoS One*. 2011;6:e25968.
27. Han X, Chen M, Wang F, et al. Forebrain engraftment by human glial progenitor cells enhances synaptic plasticity and learning in adult mice. *Cell Stem Cell*. 2013;12:342-353.
28. Krencik R, Weick JP, Liu Y, et al. Specification of transplantable astroglial subtypes from human pluripotent stem cells. *Nat Biotechnol*. 2011;29:528-534.
29. Rothstein JD, Van Kammen M, Levey AI, et al. Selective loss of glial glutamate transporter GLT-1 in amyotrophic lateral sclerosis. *Ann Neurol*. 1995;38:73-84.
30. Bristol LA, Rothstein JD. Glutamate transporter gene expression in amyotrophic lateral sclerosis motor cortex. *Ann Neurol*. 1996;39:676-679.

31. Bendotti C, Tortarolo M, Suchak SK, et al. Transgenic SOD1 G93A mice develop reduced GLT-1 in spinal cord without alterations in cerebrospinal fluid glutamate levels. *J Neurochem.* 2001;79:737-746.
32. Doi A, Park IH, Wen B, et al. Differential methylation of tissue- and cancer-specific CpG island shores distinguishes human induced pluripotent stem cells, embryonic stem cells and fibroblasts. *Nat Genet.* 2009;41:1350-1353.
33. Ohi Y, Qin H, Hong C, et al. Incomplete DNA methylation underlies a transcriptional memory of somatic cells in human iPS cells. *Nat Cell Biol.* 2011;13:541-549.
34. Zhao T, Zhang ZN, Rong Z, et al. Immunogenicity of induced pluripotent stem cells. *Nature.* 2011;474:212-215.
35. Chin MH, Pellegrini M, Plath K, et al. Molecular analyses of human induced pluripotent stem cells and embryonic stem cells. *Cell Stem Cell.* 2010;7:263-269.
36. Bock C, Kiskinis E, Verstappen G, et al. Reference Maps of human ES and iPS cell variation enable high-throughput characterization of pluripotent cell lines. *Cell.* 2011;144:439-452.
37. Osafune K, Caron L, Borowiak M, et al. Marked differences in differentiation propensity among human embryonic stem cell lines. *Nat Biotechnol.* 2008;26:313-315.
38. Hu BY, Weick JP, Yu J, et al. Neural differentiation of human induced pluripotent stem cells follows developmental principles but with variable potency. *Proc Natl Acad Sci U S A.* 2010;107:4335-4340.

Table 1. Stem cell lines used for rat spinal cord transplantation (n=number of rats receiving transplant of various cell lines).

Cell Line	Cell Type	Reference	Age	Sex	Weeks until sacrifice (n)		
					2 wks	7 wks	12 wks
H13	hESC	Cowan et al., 2004	0	M	2	2	3
11a	hiPSC	Boulting et al., 2011	36	M	2	3	3
18c	hiPSC	Boulting et al., 2011	48	F	2	3	3

SUPPORTING INFORMATION

Supporting Figure Legends

Figure S1. Characterization of hESC- and hiPSC-derived astrocyte progenitors at 2 weeks post-transplantation. **(A-C)** Human ESC- (A) and iPSC- (B-C) derived astrocyte progenitors can be localized by human nuclear antigen (HuNA) and many express GFAP *in vivo*. **(D)** Rostral-caudal cell migration from the injection (Inj.) site was measured at 2 week post-transplantation by calculating the percent of total HuNA⁺ cells along the distance of the spinal cord. Scale bars=50 µm.

Figure S2. Characterization of hESC- and hiPSC-derived astrocyte progenitors at 7 weeks post-transplantation. **(A-C)** Human ESC- (A) and iPSC- (B-C) derived astrocyte progenitors can be localized by human nuclear antigen (HuNA) and many express GFAP *in vivo*. **(D)** Rostral-caudal cell migration from the injection (Inj.) site was measured at 7 week post-transplantation by calculating the percent of total HuNA⁺ cells along the distance of the spinal cord. Scale bars=50 µm.

Figure S3. *In vivo* differentiation of hESC- and hiPSC-derived astrocyte progenitors after transplantation. **(A)** The percent of HuNA⁺ cells that also express GFAP, Olig2, or Tuj1 was quantified at 7 weeks post-transplantation. Not detected, N.D. **(B)** Transplanted HuNA⁺ cells do not express the neuronal marker Tuj1⁺ although they reside in close proximity to endogenous rat Tuj1⁺ neurons. Scale bar=10 µm.

Figure S4. Analysis of transplanted hiPSC-derived astrocyte progenitors for expression of the reactive astrocyte marker, LCN2. **(A)** LCN2 reactivity is observed in the spinal cord ventral horn in human ALS patient tissue. Scale bar=50 µm. **(B)** Transplanted HuNA⁺ cells do not express the reactive astrocyte marker LCN2 *in vivo*. Scale bar=10 µm.

Figure S5. Gene profiling of human control spinal cords (SC) from three individuals. **(A, B)** Gene profiling for astrocyte lineage (A) and non-astrocyte lineage (B) genes was assessed using Nanostring® technology.

Figure S6. Gene profiling of hESC- and hiPSC-derived astrocytes progenitors *in vitro* just prior to transplantation. **(A, B)** Gene profiling for astrocyte lineage (A) and non-astrocyte lineage (B) genes was assessed using Nanostring® technology.

Supporting Methods

iPSC culture and differentiation. Human ES and hiPS cells were maintained undifferentiated in WiCell medium composed of DMEM:F12 medium supplemented with 100 µM non-essential amino acids (Gibco), 2 mM L-glutamine, 110 mM β-mercaptoethanol (Sigma-Aldrich), 20% Knock-out serum (Millipore), and 20 ng/ml FGF2 (Invitrogen, PHD-02663). To generate ventralized spinal cord from hESCs and hiPSCs, we used previously described protocols¹⁻³ with some modifications described previously (Roybon et al, *in press*). Briefly, hESC and hiPSC colonies were detached from irradiated fibroblasts using dispase, washed three times with FGF2-free WiCell medium, and incubated for 30 minutes to 1 hour in WiCell medium supplemented with 20 ng/ml FGF2 (R&D) and 20 µM ROCK inhibitor (Y-27632; Ascent Scientific, ASC-129). Colonies were then mechanically dissociated and cell suspensions filtered through a cell strainer. Cells were seeded at 30,000-40,000 cells/cm² in WiCell medium supplemented with FGF2 (20 ng/ml) and Y-27632 (20 µM). Once confluent layers were formed, medium was switched to WiCell medium supplemented with SB431542 (10 µM, Sigma-Aldrich-Aldrich) and LDN193189 (0.2 µM, Stemgent) to neuralize the cultures. This was considered day 1 of differentiation. At day 3, retinoic acid (RA, 1 µM, Sigma-Aldrich) and ascorbic acid (0.4 µg/ml, Sigma-Aldrich), were added. At day 7, rhBDNF (10 ng/ml, R&D) and sonic hedgehog (SHH-C, 200 ng/ml, Invitrogen) were added. At day 10, monolayers, which at this stage are mainly composed of Pax6+ neuroepithelial cells, were passaged onto 100 µg/mL poly-ornithine /

15 µg/ml laminin-coated surfaces. Monolayers of neural progenitors were cultured in 100% NIM (neural induction medium) with the addition of Y-27632 to prevent cell death. At day 15, medium was switched to NIM:NDM medium (1:1 v/v) supplemented with 1 µM RA, SHH-C (200 ng/ml), 2% B27 (Millipore), rhBDNF, rhGDNF, rhIGF and rhCNTF (all at 10 ng/ml; R&D Systems). On day 21, we used the same supplements in 100% NDM for 10 additional days. To generate astrocytes, at day 31, cultures were passaged onto 100 µg/mL poly-ornithine / 3-5 µg/ml laminin-coated surfaces in NS medium supplemented with 1% FBS. Cultures were passaged when they reached confluence. After 90 days of differentiation, astrocytes were frozen for storage and then thawed just prior to transplantation.

Tissue Processing and IHC: Animals were sacrificed at 2, 7, and 12 weeks post-transplantation. Animals were anesthetized with 4% chloral hydrate and perfused with 0.9% saline, followed by ice-cold 4% paraformaldehyde (Fisher). Spinal cords were removed from the animal, followed by cryoprotection in 30% sucrose (Fisher)/0.1 M phosphate buffer at 4°C for 3 days. The tissue was embedded in Tissue Freezing Media (Triangle Biomedical Sciences), fast frozen with dry ice, and stored at -80°C until processed. Spinal cord tissue blocks were cut in the transverse planes at 30 µm thickness. Sections were collected on glass slides and stored at -20°C until analyzed.

Immunohistochemistry. For *in vitro* cell fixation, cells were fixed in 4% PFA for 10 min, and then washed with TBS three times. Tissue was blocked for 1 hr. in 10% goat serum with 0.3% triton-X then probed overnight with primary antibody at 4°C in 2% goat serum with 0.3% triton-X. Tissue sections were washed in TBS then incubated with secondary antibody (Alexa Fluor, Life Technologies at 1:1000 or Jackson Immunoresearch at 1:200) for 2 hrs. at room temperature followed by further washing in TBS. Tissue sections were mounted with Prolong Gold with DAPI (Life Technologies). Primary antibodies used: Human nuclear antigen (HuNA) (Millipore #MAB1281, 1:100), human mitochondria (hMito) (Millipore #MAB1273, 1:100), Aquaporin4 (Millipore #AB3594, 1:100), (Tuj1 (Covance #MRB-435P, 1:500), Glial Fibrillary Acidic Protein

(GFAP) (DAKO #Z0334, 1:400), GFAP (Millipore #AB5541, 1:200), Olig2 (Millipore #AB9610, 1:500), Nestin (Millipore #AB5922, 1:1000), CD44 (BD Pharmingen #550392 1:100), LCN2 (Abnova #PAB6795, 1:200). Images were acquired on either a Zeiss fluorescence microscope using a Photometric Sensys KAF-1400 CCD camera (Roper Scientific) or on a Zeiss laser confocal microscope. Transplanted cells were localized by staining for human nuclear antigen (HuNA) antibody (to identify human cells in rat spinal cord). To estimate the total number of surviving cells, total numbers of HuNA⁺/DAPI⁺ cells were quantified in every 6th section throughout the extent of transplanted spinal cord as we have previously done.^{4,5} HuNA⁺/DAPI⁺ cells from these sections were summed and multiplied by 6 to estimate the total number of surviving cells. Values were expressed as a percentage of the total number of cells transplanted.

1. Boultling GL, Kiskinis E, Croft GF, et al. A functionally characterized test set of human induced pluripotent stem cells. *Nat Biotechnol.* 2011;29:279-286.
2. Chambers SM, Fasano CA, Papapetrou EP, et al. Highly efficient neural conversion of human ES and iPS cells by dual inhibition of SMAD signaling. *Nat Biotechnol.* 2009;27:275-280.
3. Li XJ, Du ZW, Zarnowska ED, et al. Specification of motoneurons from human embryonic stem cells. *Nat Biotechnol.* 2005;23:215-221.
4. Lepore AC, O'Donnell J, Kim AS, et al. Human glial-restricted progenitor transplantation into cervical spinal cord of the SOD1 mouse model of ALS. *PLoS One.* 2011;6:e25968.
5. Lepore AC, Rauck B, Dejea C, et al. Focal transplantation-based astrocyte replacement is neuroprotective in a model of motor neuron disease. *Nat Neurosci.* 2008;11:1294-1301.

Table S1. Targeted genes and sequences used in Nanostring® probe design.

	Gene	Accession Number	Target Region	Target Sequence
1	GFAP	NM_002055.4	756-856	CTCACCGCAGCCCTGAAAGAGATCCGCACGCAGTATGAGGCAATGGCGTCAGCAACATGCATGAAGCGAAGAGTGGTACCGCTCCAAGTTGCAGACC
2	AQP4	NM_004028.3	2520-2620	CAGTTGTGTCTGTGGCAGTGAGATAATGGACCACTATTAAACCTGATTCTCTCGGTGCTAGGAAAGAGTGATGTGAGATTCCCAGAGAGTCGTCA
3	PLA2G7	NM_005084.3	255-355	GCTCAGCTCCCAAGATGGTGCCACCCAAATTGCATGTGCTTTCTGCCTCTGCAGCCTGGCTGGCTGTGGTTATCCTTTGACTGGCAATACATAAAATCC
4	SLC39A12	NM_001145195.1	883-983	CGCTTCCTCAGTTGGCAGCCATGATCATTACTTGTCCCTCCAGGGTGTGCTGGGACAAAGAGAAACTTGCCTCCCCAGACTACTTACAGAATATAT
5	MLC1	NM_015166.3	1830-1930	CCCTAACATGCCCTGAGCTACTGCTTAACACCTCTTCCCTGTGAGGGCAAACAGGCTGCAGGTGGGGTTTCACCTCTAGGGTAGTTAATT
6	DIO2	NM_013989.3	5075-5175	TATGTATGCCTTCGGGAAAATTCAAAGGTGGATTACAAGGGTGCCTCAGCATGCCCTATGGCCTATGTGCGAAGCAAGAATTGACTGATTACAGGA
7	SLC14A1	NM_015865.1	730-830	TTTCAGCCACAGGACATTACAATCCGTTCTTCCAGCCAAACTGGTCATAACCTATAAC TACAGCTCCAAATATCCTCTGGTCTGACCTCAGTGCCCTGGA
8	ALDH1L1	NM_012190.2	329-429	AGAAGGATGGAGTGCCGGTATTCAAGTACTCCCGTGGCGTGCAAAAGGACAGGC TTGCGCTGATGTGGTGGCAAAATACCAAGGCTTGGGGGCCAGCT
9	ALDOC	NM_005165.2	1521-1621	ATGAGGTAGCTTCCCTGGCTCCTCTTGCCCTGCCCTGTCTCCTGGGATCAGAGGGTAGTACAGAAGCCCTGACTCATGCCCTGAGTACATACCAT
10	TTPA	NM_000370.3	1656-1756	ATTACAGTCGTGAGCCATCGCGCTGGCCGTGATAGAAACTTCAGCTGAGGAGTC TATATGCCATACTACTCTATGTGGCATCTTAGGTCTCTGTGAA
11	ACSBG1	NM_001199377.1	2604-2704	AGGTGACAAATGAGATCAGCTCCCTCCAGAACGAAAGGGCTGATAATTGGCC TTAGTTCCAGGTAGATTAAGCTGCTAGCTCACATACAGGA
12	CHRD1	NM_001143981.1	3539-3639	CAGAGGTGGCAGTGATTCCATAATGTGGAGACTAGTAACTAGATCCTAAGGCAAAGAGGTGTTCTCCTCTGGATGATTCACTCCAAAGCCTCCCACC
13	SLC4A4	NM_001098484.2	4653-4753	GTGCTCTGTGCCATGGCTGGTATATATGTCAATGTTAGAAGGCAAAGAGTGATGGTAGGCAGAGGGCAAAGTCATTGAATCTTATGCCAGTTTT
14	Slc1a2	NM_004171.3	6360-6460	TGACTAAAAGTGCACAGCAGTTATACCCAGTGGAAAGTGATTTCTCACCTAGCTGCTCTCTAACTCTTACGGCTATCTAGTTGTCTGAGCTGCTGGTT
15	Slc25a18	NM_031481.1	1575-1675	GGAGAAACAGCCCTATATTCTAACAAAGTTGAGCAGCACAGCCTCTCCCTCGTGTCTACACTCGTTCTGAGGACAGCTACCAGGGCTTGG
16	SLC1A3	NM_0041	558-	TGGCCAAGAAGAAAGTGCAGAACATTACAAAGGAGGATGTTAAAGTTACCTGTTCTG

		72.4	658	GGAATGCTTTGTGCTGCTCACAGTCACCGCTGTCAATTGTGGG
17	F3	NM_0019 93.3	1030- 1130	GAGCTGGAAGGAGAACTCCCCACTGAATGTTCATAAAGGAAGCACTGTTGGAGCT ACTGCAAATGCTATATTGCACTGTGACCGAGAACCTTAAGAGG
18	FZD2	NM_0014 66.3	2653- 2753	CCCCTGCAGGCTGGAAGATCTTCTCCTGTCTGGCTCTCTCTTCAATTGCTG CACCAAGTGCTCCAGTGGCCAAAATGCTTTGAAGTGTG
19	MERTK	NM_0063 43.2	2675- 2775	CTGCAGCTAGAAAAACTCTTAGAAAGTTGCCTGACGTTCGGAACCAAGCAGACGTT ATTACGTCAATACACAGTTGCTGGAGAGCTCTGAGGGCCTGG
20	EZR	NM_0033 79.4	2165- 2265	ATAGTGCCAAGCAGGCCTGATTCTCGCGATTATTCTCGAATCACCTCCTGTGTTGTG CTGGGAGCAGGACTGATTGAATTACGGAAAATGCCTGTAAAGT
21	Top2a	NM_0010 67.2	5376- 5476	TTTCAGCTCTTGACCTGTCCTCTGGCTGCCTCTGAGTCTGAATCTCCAAAGAGA GAAACCAATTCTAAAGAGGACTGGATTGCAAGAACACTGGGGA
22	Aurkb	NM_0042 17.2	615- 715	AGATGCTCTAATGTAUTGCCATGGGAAGAAGGTGATTCACAGAGACATAAGCCAG AAAATCTGCTCTAGGGCTCAAGGGAGAGCTGAAGATTGCTGAC
23	CDK1	NM_0017 86.4	162- 262	AGAGAAAATTGGAGAAGGTACCTATGGAGTTGTGTATAAGGGTAGACACAAAATAC AGGTCAAGTGGTAGCCATGAAAAAAATCAGACTAGAAAGTGA
24	Pbk	NM_0184 92.2	1587- 1687	GCTGATGTGTTATCAAATGATAACTGGAAGCTGAGGGAGAATATGCCCTAAAAAGAG TAGCTCCTGGACTTCAGACTCTGGTACAGATTGTCTTGA
25	Emp1	NM_0014 23.1	2000- 2100	AGCAAAAACCTTGTGGTACCTAGTCAGATGGTAGACGAGCTGTCTGCCGCAG GAGCACCTCTATACAGGACTTAGAAGTAGTATGTTATTCTGGT
26	Sult1a1	NM_1775 34.2	1393- 1493	TGCGAATCAAACCTGACCAAGCGGCTCAAGAATAAAATGAATTGAGGGCCCGGG ACGGTAGGTATGTCTGTAATCCCAGCAATTGGAGGCTGAGGT
27	Dmp1	NM_0010 79911.2	85-185	AGAGGTATCACACCCAACATGAAGATCAGCATCCTGCTCATGTTCCCTGGGGATT ATCCTGTGCTCTCCAGTAACCAGGTATCAAATAATGAATCT
28	RCAN2	NM_0058 22.3	2767- 2867	GTGTCTCTAGTGGAGAAAATAGTAGGCTCCGCTATTCACTGAGTCAGAGCACTGCAG CATCCAGCCTTCAAAGCTGACTCTCAATCATCTGTGGTC
29	Clmn	NM_0247 34.3	3335- 3435	TACTAAAACTCAGGCATGCAGCTGGATCCGTAGGTGGGGTTTGTCTTGTGTC CTTGCTGGTTGGATAGGGAGCATTGTTAGTGTACATTAGCCCG
30	PTGER4	NM_0009 58.2	2302- 2402	GCGAAGACCTACCCCTCCGTTTCTACTAGATAGGAGGATGGTAGAAGTTGGCTGC TGTCTACAACATCCAGAGCTTGTGCTATTGGCACACAGCAGA
31	Igfbp3	NM_0005 98.4	1255- 1355	TATCAAAATATTCAAGAGACTCGAGCACAGCACCCAGACTTCATGCCCGTGAAT GCTCACCAACATGTTGGTGAAGCGGCCGACCACTGACTTTGTGA
32	Spp1	NM_0005 82.2	760- 860	CGCCTTCTGATTGGGACAGCCGTGGGAAGGGACAGTTATGAAACGAGTCAGCTGGAT GACCAGAGTGCTGAAACCCACAGCCACAAGCAGTCCAGATTATA
33	Anxa3	NM_0051 39.2	1020- 1120	AGACTTACTGTTGGCCATAGTTAATTGTGTGAGGAACACGCCGCCCTTTAGCCGA AAGACTGCATCGAGCCTGAAAGGGTATTGGAACTGATGAGTT

34	Anxa1	NM_0007 00.1	577- 677	AACCTCAGACACATCTGGAGATTTCGGAACGCTTGCTTCTTGCTAAGGGTGA CCGATCTGAGGACTTGGGTGAATGAAGACTGGCTGATTCA
35	CFH	NM_0010 14975.2	702- 802	GGAAAAATTGTCAGTAGTGCATGGAACCAGATCGGGATACCATTGGACAAGCA GTACGGTTGTATGTAACCTCAGGCTACAAGATTGAAGGGAGATG
36	NES	NM_0066 17.1	2345- 2445	CAGAGAACATCACAAATCACTGAGGTCTTAGAAGAACAGGACCAAGAGACATTGAGAA CTCTGAAAAAGAGACTCAACAGCGACGGAGGTCTAGGGGA
37	SOX2	NM_0031 06.2	151- 251	CTTAAGCCTTCCAAAAATAATAACAATCATCGCGGCCAGGATCGGCCAG AGGAGGAGGGAAAGCGCTTTTGATCCTGATTCCAGTTGCC
38	PDGFRA	NM_0062 06.3	1925- 2025	TAGTGCTTGGTCGGGTCTGGGGCTGGAGCGTTGGGAAGGTGGTTGAAGGAACA GCCTATGGATTAAGCCGGTCCAACCTGTATGAAAGTTGCAGT
39	CNP	NM_0331 33.4	1575- 1675	CGCCCTCTCCCCCTCAATGCTCACGCTCCAACACAAGGTGGGCAGGGAGGCACC ATTCAAGGAACCTGGACCAAAGCTGACGAGGCTGGGCCAACGCCAG
40	MOG	NM_0010 08228.2	662- 762	AAGATCCTTCTACTGGGTGAGCCCTGGAGTGCTGGTTCTCCTCGCGGTGCTGCCT GTGCTCCCTGCAGATCACTGTTGGCCTCATCTCCTCTGCCT
41	OLIG2	NM_0058 06.2	1690- 1790	TAGTTGGAAGCCGGCGTCGGTATCAGAACCGCTGATGGTATATCCAATCTCAATA TCTGGGTCAATCCACACCCTCTAGAACTGTGGCCGTTCCCTCC
42	CD44	NM_0010 01392.1	429- 529	ACACCATGGACAAGTTGGTGGCACGCAGCCTGGGACTCTGCCTCGTGGCGCT GAGCCTGGCGCAGATCGATTGAATATAACCTGCCGTTGCAGG
43	S100B	NM_0062 72.1	85-185	AGAAGGCCATGGTGGCCCTCATGCACGTTCCACCAATATTCTGGAAGGGAGGG GACAAGCACAAGCTGAAGAAATCCGAACTCAAGGAGCTCATCAA
44	Connexin 43	NM_0001 65.3	2736- 2836	GAGTTAGCAGTCTTGAGTGACCAACTTGATGTTGCACTAAGATTATT TGGAATGCAAGAGAGGTTGAAAGAGGATTCACTAGTAGTACACAT
45	TUBB3	NM_0060 86.2	1537- 1637	GCCGCCCTCCTGCAGTATTATGGCCTCGCCTCCCCACCTAGGCCACGTGTGAGC TGCTCCTGTCTGTCTTATTGCAGCTCCAGGCCTGACGTTTA
46	NEUROD6	NM_0227 28.2	377- 477	TCTGTTGTAATGCCAGAACCCAGATGTGCAGAAAGTTCTAGAGAACGCGAGGAC CAGAACGAAATTAGAACGCCAGAAAGCTTTCCAACAGATTG
47	ITGAM	NM_0006 32.3	515- 615	GCCCTCCGAGGGTGTCTCAAGAGGATAGTGACATTGCCTCTGATTGATGGCTC TGGTAGCATCATCCCACATGACTTCCGGCGATGAAGGAGTTG
48	GAPDH	NM_0020 46.3	104- 204	GGGGAAAGGTGAAGGTCGGAGTCACGGATTGGTCGTATTGGCGCTGGTCACC AGGGCTGCTTTAACCTCTGGTAAAGTGGATATTGTTGCCATCAAT
49	B2M	NM_0040 48.2	25-125	CGGGCATTCTGAAGCTGACAGCATTGGGCCAGAGATGTCCTCGCTCCGTGGCCTTA GCTGTGCTCGCGCTACTCTCTTCTGGCCTGGAGGCTATCCA
50	GUSB	NM_0001 81.1	1350- 1450	CGGTCTGATGTGGTCTGTGGCCAACGAGCCTGCCTCCACCTAGAACCTGCTGGC TACTACTGAAAGATGGTATCGCTCACACCAAATCCTGGACCC
51	OAZ1	NM_0041 52.2	313- 413	GGTGGCGAGGGAAATAGTCAGAGGGATACAATCTTCAGCTAACCTATTACTCC GATGATCGGCTGAATGTAACAGAGGAACAAACGTCCAACGACA

Table S2. Gene profiling of transplanted human cells *in vivo* in cervical and lumbar spinal cord sections (raw counts).

Gene	Accession Number	18c C3	18c C4	18c C5	18c C6	18c C7	18c L1	11a C3	11a C4	11a C5	11a C6	11a C7	11a L1	H13 C3	H13 C4	H13 C5	H13 C6	H13 C7	H13 L1
GFAP	NM_002055.4	41	64	4268	37	25	24	31	37	784	1277	31	24	1	42	818	3067	69	16
AQP4	NM_004028.3	7	11	259	12	2	1	2	4	134	171	5	4	1	2	82	298	5	2
MLC1	NM_015166.3	3	6	130	4	1	1	3	2	14	32	1	2	5	4	57	151	12	2
Slc1a2 (EAAT2)	NM_004171.3	3	3	41	5	1	1	4	3	5	2	1	2	3	2	14	12	16	3
SLC1A3 (EAAT1)	NM_004172.4	226	187	359	157	157	224	228	277	322	350	226	272	4	305	470	668	323	218
NES (Nestin)	NM_006617.1	1	4	155	12	7	1	1	2	26	18	1	2	1	1	40	120	22	2
SOX2	NM_003106.2	5	10	117	7	5	8	3	2	23	22	4	3	5	6	40	116	18	5
PDGFRA	NM_006206.3	12	11	36	8	12	9	12	12	19	9	12	10	9	16	50	71	44	12
CNP	NM_033133.4	5	1	28	5	2	7	1	3	2	10	2	2	1	3	15	27	18	2
MOG	NM_001008228.2	1	1	5	1	1	4	2	2	1	3	3	1	1	1	1	1	1	2
OLIG2	NM_005806.2	2	1	24	4	2	1	2	2	3	5	3	2	1	11	66	127	94	1
CD44	NM_001001392.1	99	107	282	90	103	71	67	58	93	96	61	60	6	93	131	155	114	45
S100B	NM_006272.1	22	23	111	23	9	16	21	21	103	165	29	22	9	25	85	201	48	14
Connexin 43	NM_000165.3	2	5	608	8	1	1	4	3	97	161	2	1	1	1	153	478	8	1
TUBB3 (β -Tubulin)	NM_006086.2	9	1	12	6	1	3	5	3	6	6	7	4	1	4	7	11	7	7
NEUROD6	NM_022728.2	1	3	4	2	1	1	3	3	2	6	1	1	1	1	5	3	1	2
ITGAM (Cd11b)	NM_000632.3	1	1	1	1	1	1	1	1	1	1	1	1	1	1	1	2	1	

Table S3. Gene profiling of astrocyte progenitors *in vitro* prior to transplantation (normalized using human housekeeping genes).

Gene	Accession Number	11a	18c	H13
GFAP	NM_002055.4	276	940	1281
AQP4	NM_004028.3	ND	ND	ND
MLC1	NM_015166.3	48	111	161
Slc1a2 (EAAT2)	NM_004171.3	10	12	ND
SLC1A3 (EAAT1)	NM_004172.4	170	300	1259
NES (Nestin)	NM_006617.1	4064	6139	5851
SOX2	NM_003106.2	752	1462	1286
PDGFRA	NM_006206.3	45	215	74
CNP	NM_033133.4	660	707	1263
MOG	NM_001008228.2	ND	ND	ND
OLIG2	NM_005806.2	ND	ND	ND
CD44	NM_001001392.1	2563	4328	6093
S100B	NM_006272.1	212	177	310
Connexin 43	NM_000165.3	17866	21823	17665
TUBB3 (β -Tubulin)	NM_006086.2	1070	1008	1460
NEUROD6	NM_022728.2	ND	ND	ND
ITGAM (Cd11b)	NM_000632.3	ND	ND	ND

ND (Not detected): Prior to normalization using human housekeeping genes, the raw count was less than 10.

Table S4. Gene profiling comparisons of astrocyte progenitors *in vitro* prior to transplantation versus *in vivo* after transplantation (normalized using human housekeeping genes).

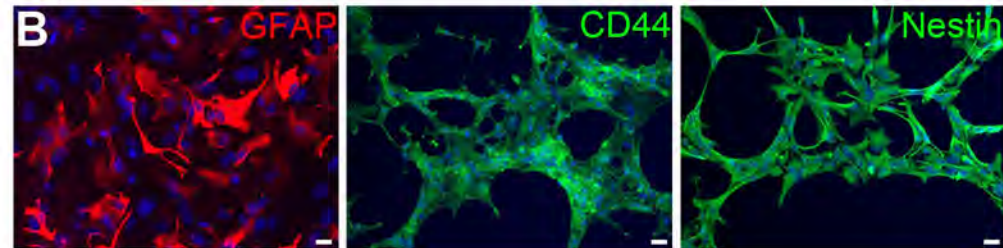
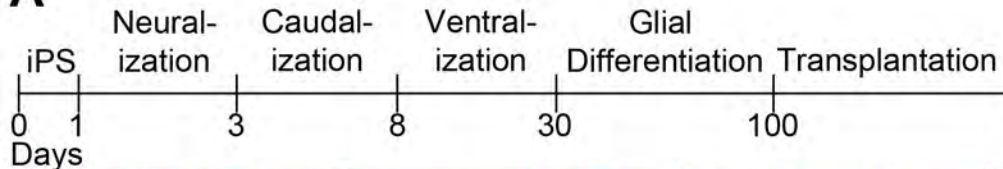
Gene	H13 <i>in vitro</i>	H13 C6	11a <i>in vitro</i>	11a C6	18c <i>in vitro</i>	18c C5
GFAP	879	120918	151	87096	547	167076
AQP4	ND	11765	ND	11649	ND	10130
PLA2G7	ND	ND	ND	ND	6	ND
SLC39A12	ND	ND	ND	ND	ND	ND
MLC1	111	5951	26	2189	65	5089
DIO2	ND	ND	12	ND	27	ND
SLC14A1	9	ND	4	235	ND	ND
ALDH1L1	14	ND	6	ND	12	471
ALDOC	ND	ND	9	ND	ND	ND
TTPA	14	ND	9	ND	13	ND
ACSBG1	247	447	5	782	36	471
CHRDL1	1047	894	1104	ND	3316	1885
SLC4A4	26	2821	21	860	11	2073
Slc1a2 (EAAT2)	ND	482	6	ND	7	1602
Slc25a18	ND	138	8	ND	13	565
SLC1A3 (EAAT1)	864	26351	93	23846	175	14041
F3	163	1101	1374	1564	530	3392
FZD2	178	ND	49	ND	51	ND
MERTK	ND	ND	ND	ND	12	ND
EZR	3471	8944	6053	8444	10193	8905
Igfbp3	1996	ND	10857	ND	11682	ND
Spp1	638	ND	750	ND	369	ND
Anxa3	558	ND	1823	ND	975	ND
Anxa1	5607	4025	4038	2502	4072	4288
CFH	123	ND	ND	ND	ND	ND
Top2a	1483	1066	229	ND	403	ND
Aurkb	745	ND	188	ND	316	ND
CDK1	1470	1170	307	ND	588	ND
Pbk	505	447	141	ND	238	ND
Emp1	251	1479	239	3127	214	3440
Sult1a1	19	344	19	ND	51	ND
Dmp1	ND	ND	ND	ND	7	ND

RCAN2	1012	ND	224	ND	329	ND
Clmn	29	ND	11	860	15	ND
PTGER4	92	ND	43	ND	40	ND

ND (Not detected): Prior to normalization using human housekeeping genes, the raw count was less than 10.

Figure 1 Maragakis et al.
Top

A



C

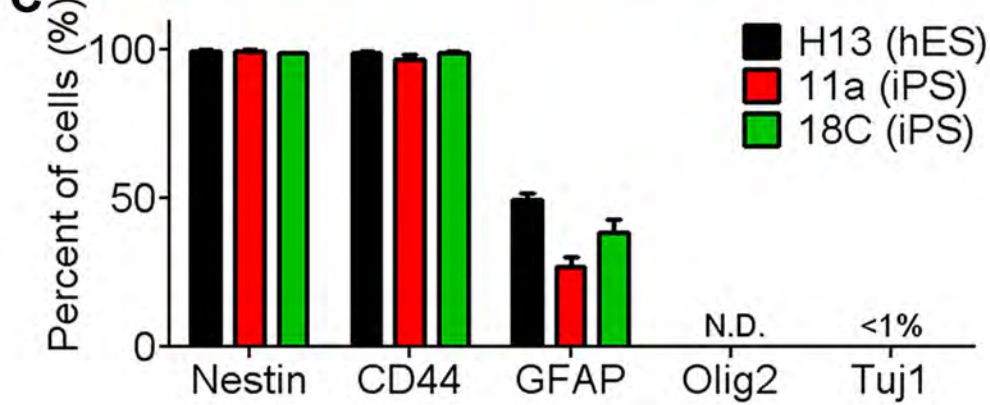


Figure 2 Maragakis et al.
Top

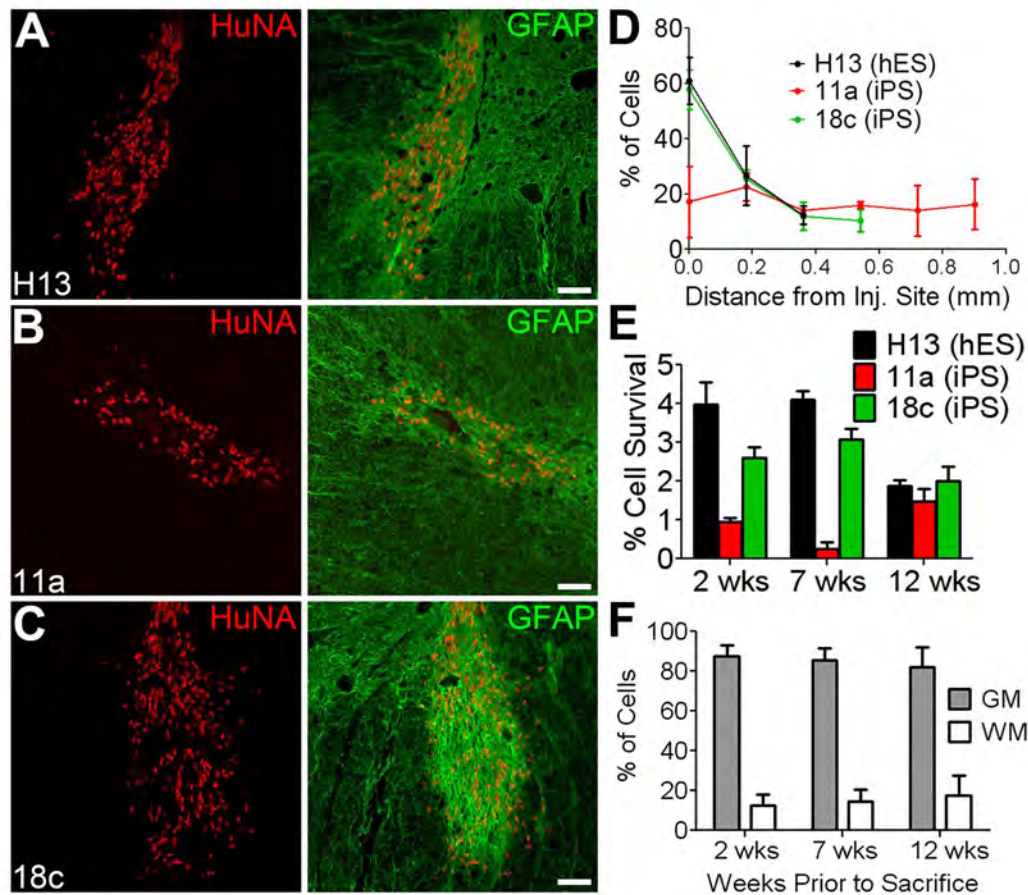


Figure 3 Maragakis et al.

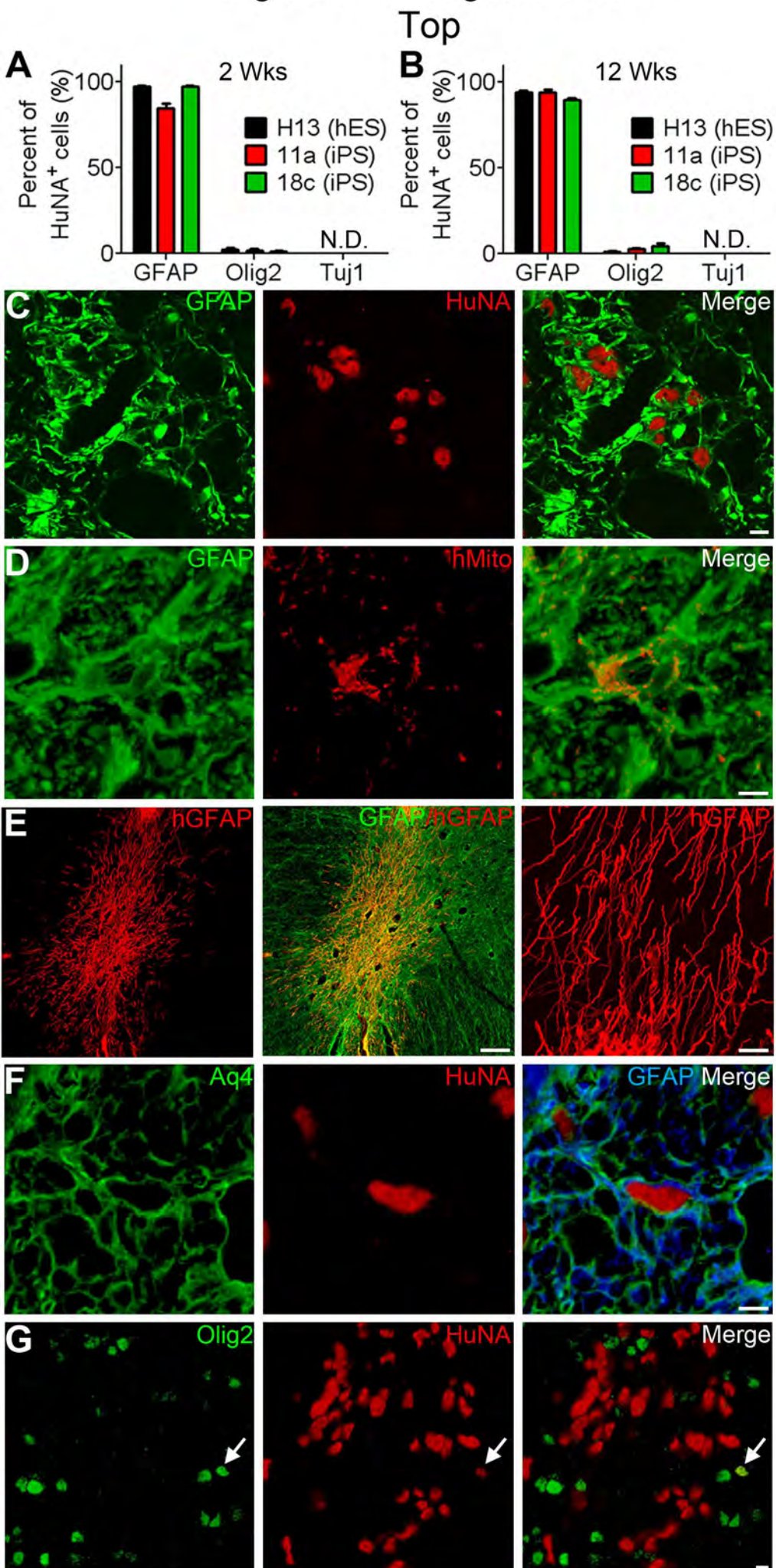


Figure 4 Maragakis et al.
Top

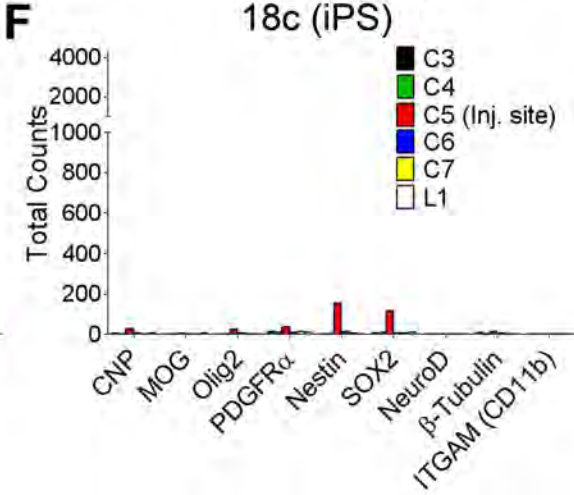
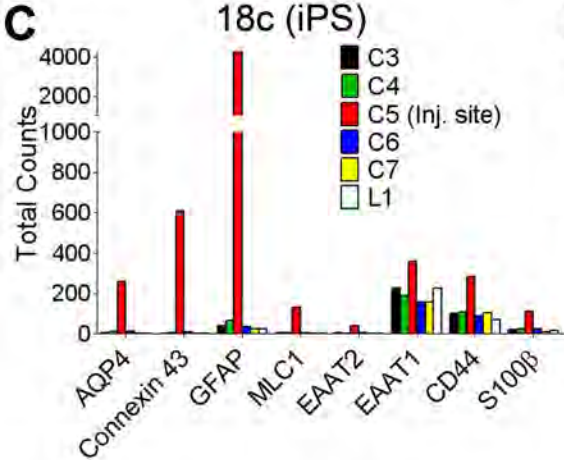
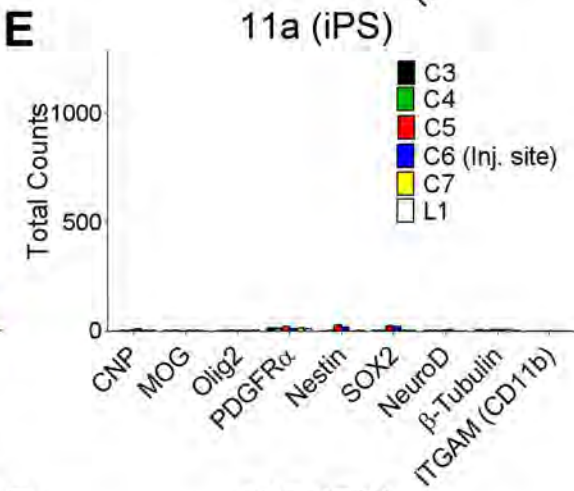
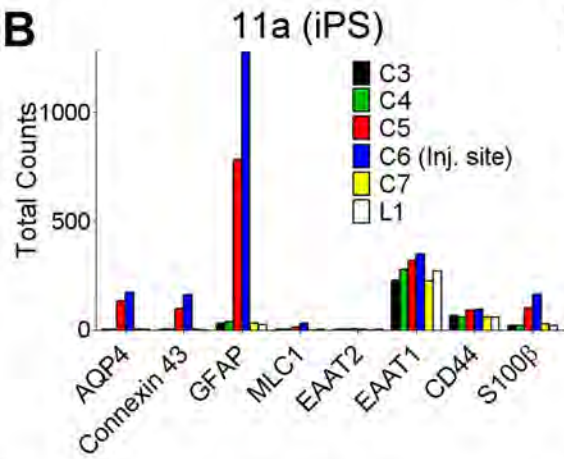
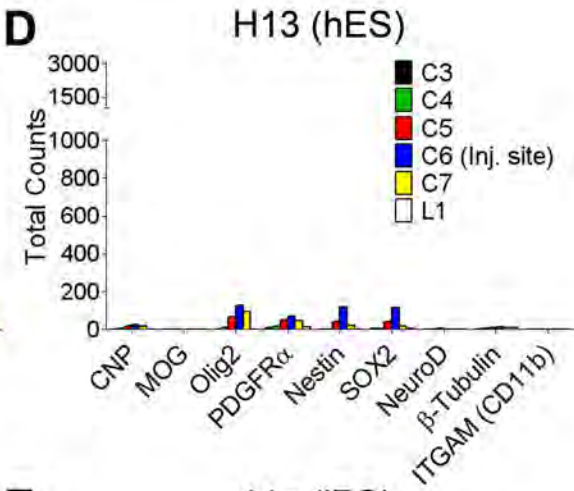
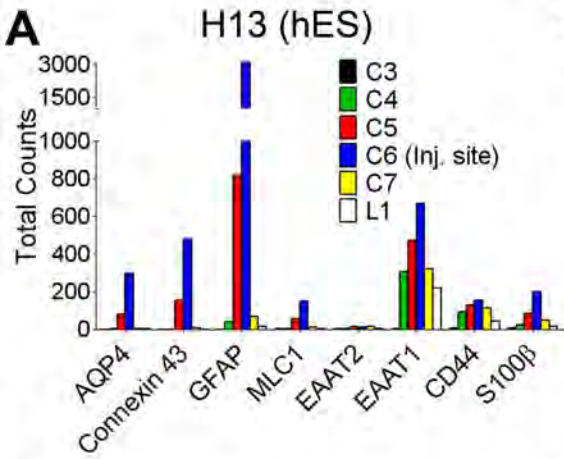
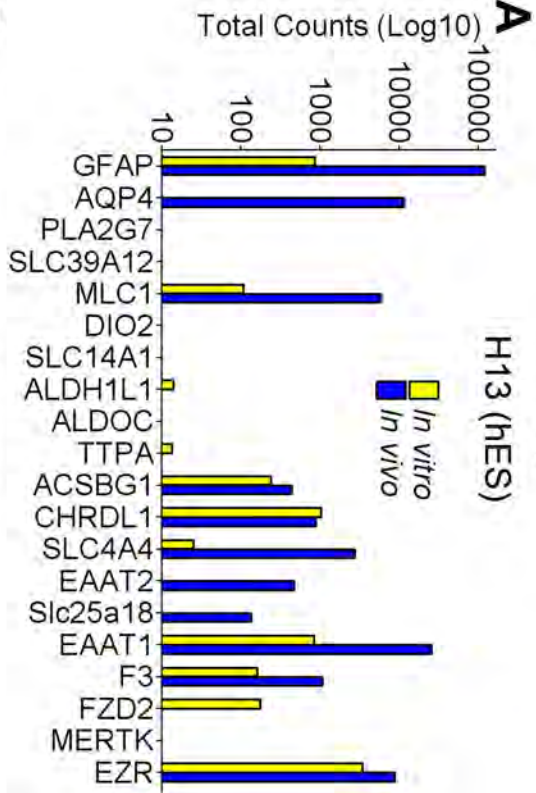
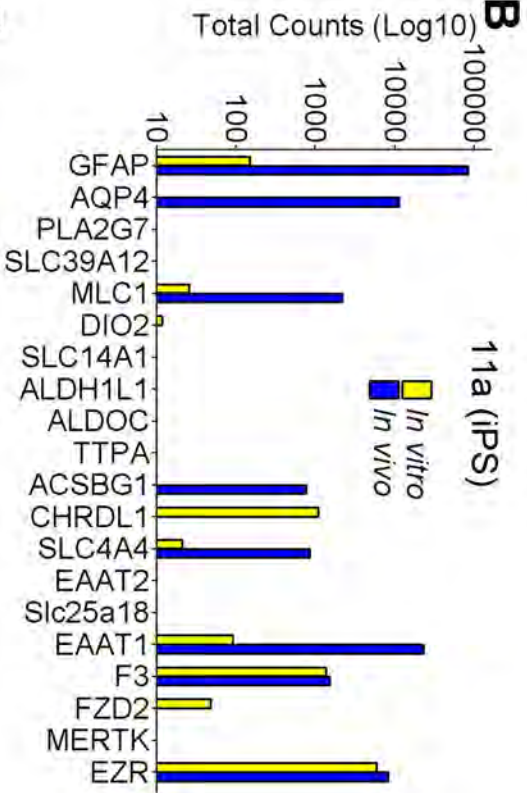


Figure 5 Maragakis et al.



11a (iPS)



18c (iPS)

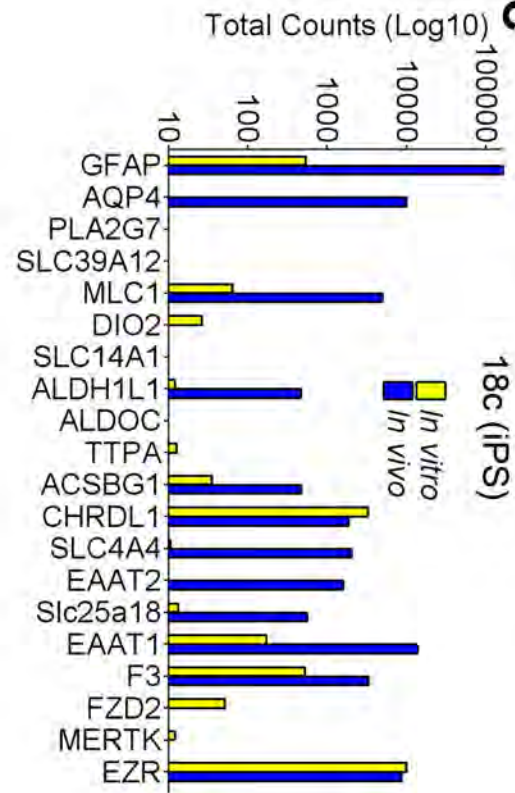


Figure 6 Maragakis et al.

Top

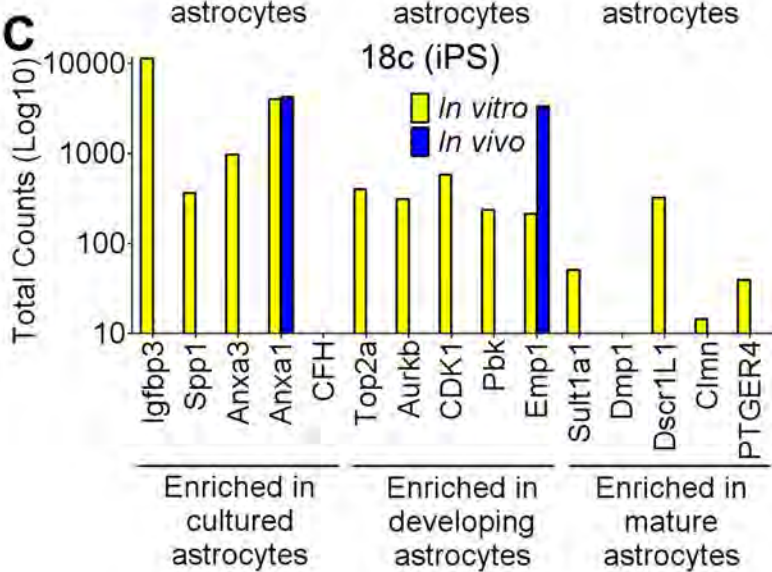
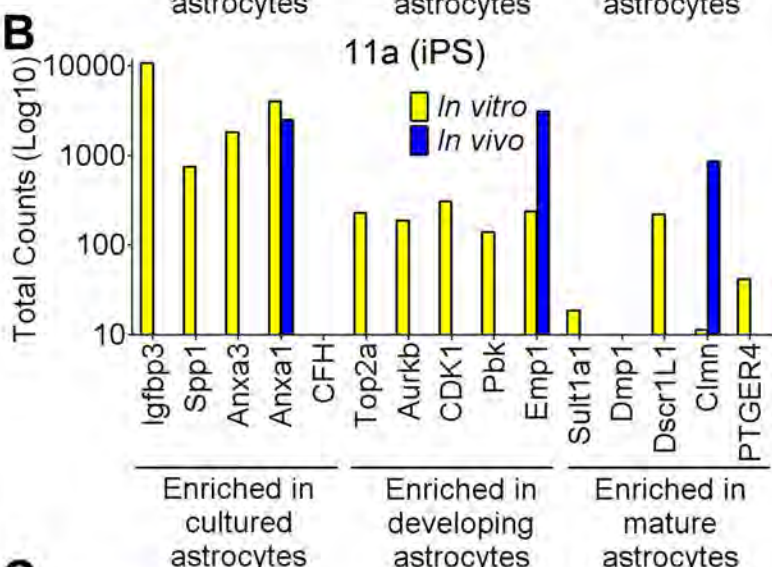
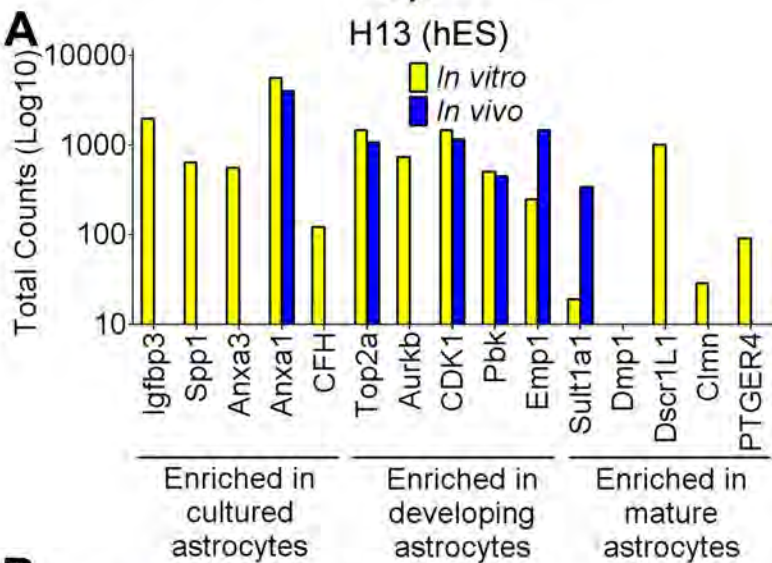


Figure S1 Maragakis et al.

Top

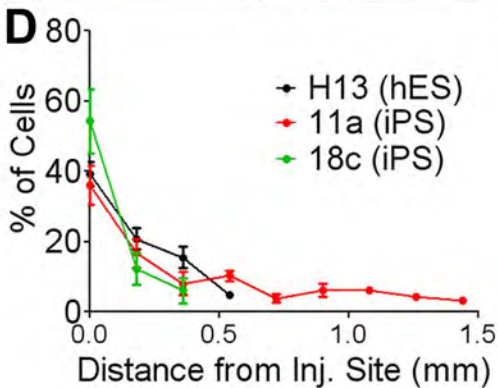
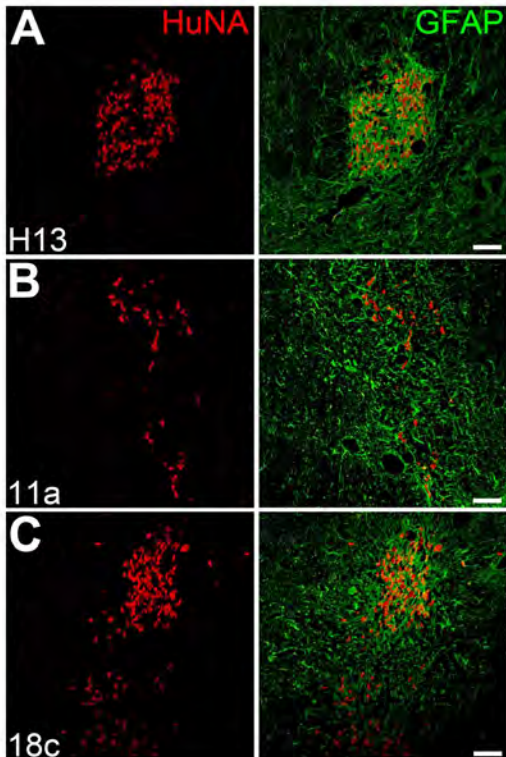


Figure S2 Maragakis et al.
Top

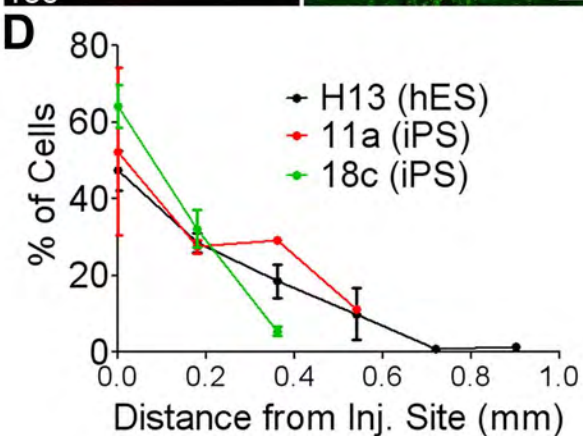
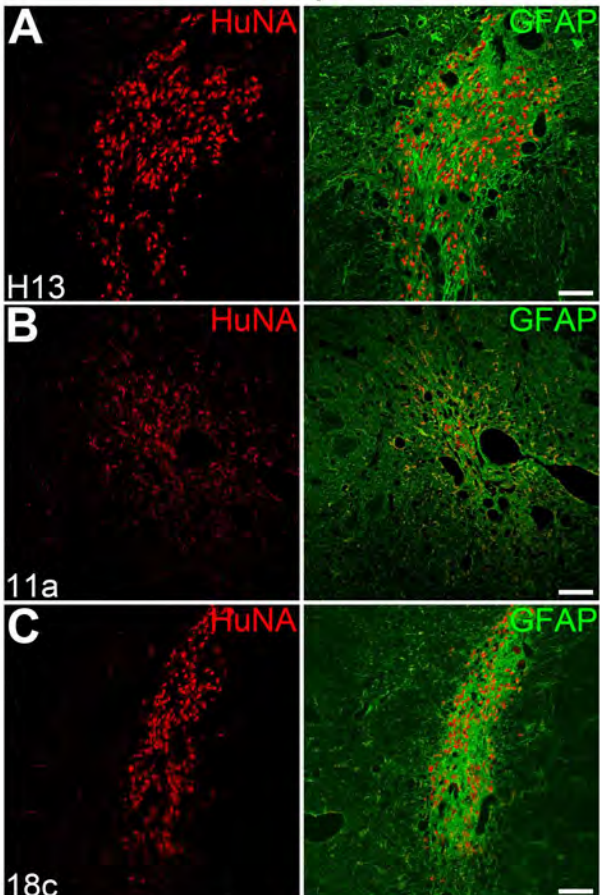


Figure S3 Maragakis et al.
Top

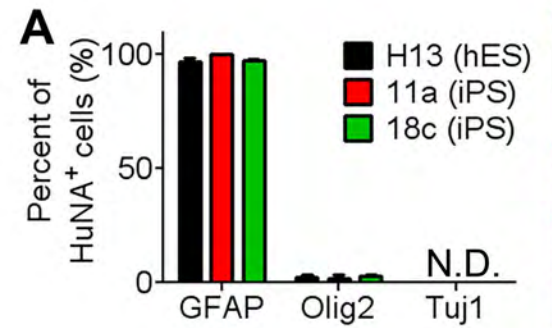


Figure S4 Maragakis et al.
Top

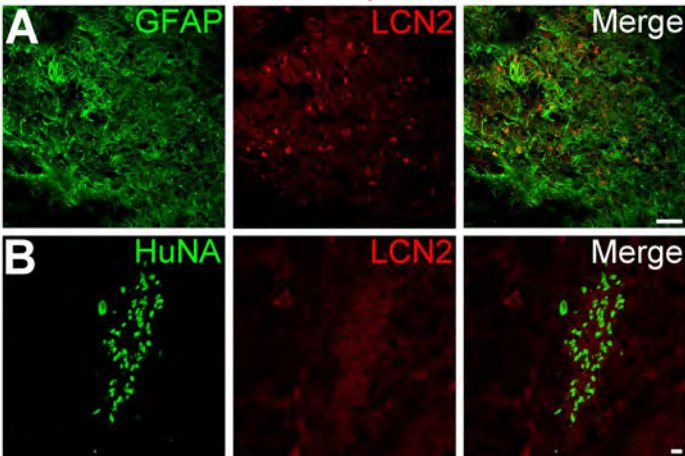
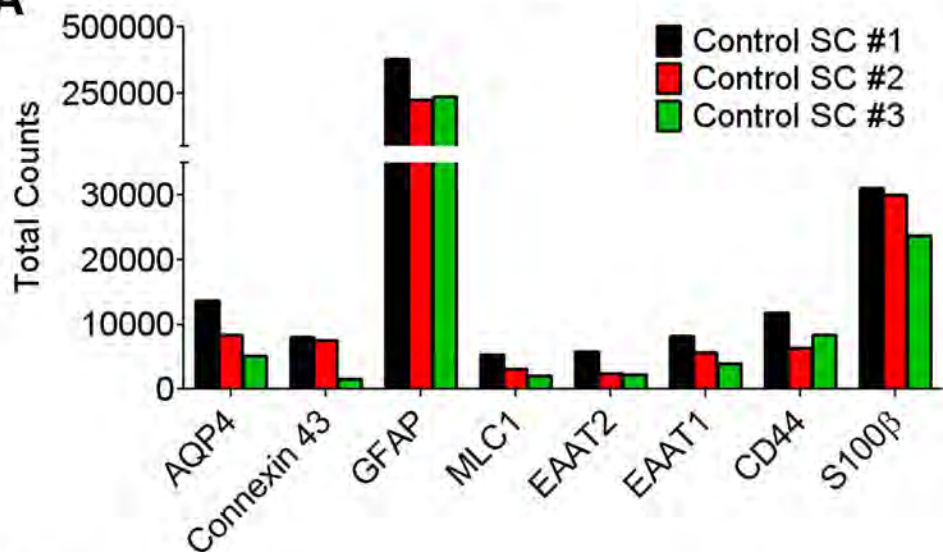


Figure S5 Maragakis et al.
Top

A



B

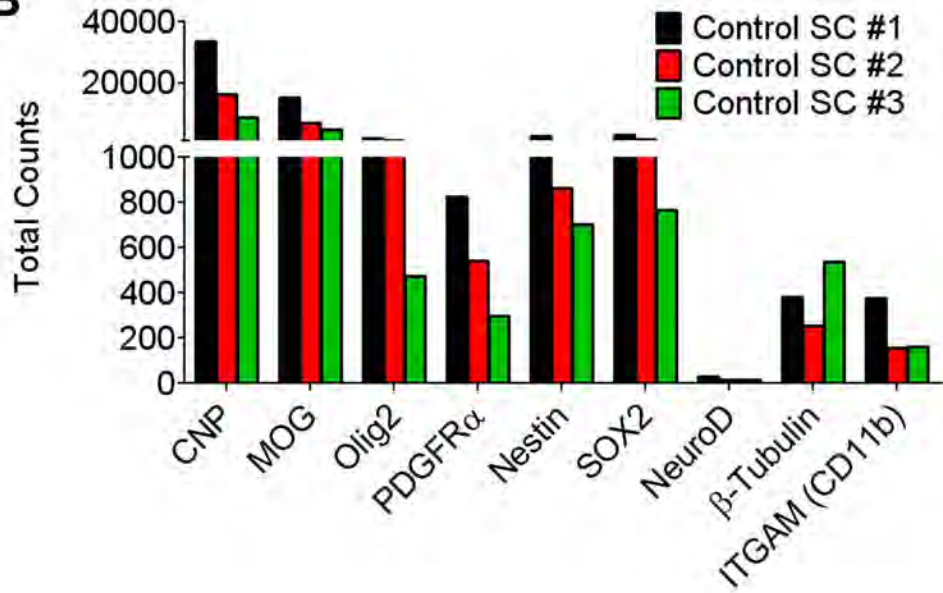


Figure S6 Maragakis et al.
Top

